Mesozoic and Cenozoic Carbonate Systems of the Mediterranean and the Middle East

Stratigraphic and Diagenetic Reference Models

Edited by
F. S. P. van Buchem, K. D. Gerdes and M. Esteban

Geological Society
Special Publication 329

Spatial and temporal distribution of ooids along a Jurassic carbonate ramp: Amellago outcrop transect, High-Atlas, Morocco

A. PIERRE[1,3,4]*, C. DURLET[1], P. RAZIN[2] & E. H. CHELLAI[3]

[1]*UMR CNRS Biogéosciences, Université de Bourgogne – 6, Boulevard Gabriel-21000, Dijon, France*

[2]*Institut EGID, Université Bordeaux III-1, allée Daguin, 33607 Pessac, France*

[3]*Faculté des Sciences Semlalia, PO Box 2390, Marrakech, Morocco*

[4]*Present address: Chevron Energy Technology Company, 6001, Bollinger Canyon Road, San Ramon, CA 94583, USA*

**Corresponding author (e-mail: aurelien.pierre@chevron.com)*

Abstract: Carbonate ramp systems are widespread throughout the geological record, but very few areas have seismic-scale, continuous and structurally undeformed outcrops that allow reliable interpretation of facies distributions and stacking patterns. The Amellago outcrop shows the detailed depositional and stratigraphic relationships of an ooid-dominated ramp system that is almost completely exposed along a dip profile (37 km long and 1000 m thick) in the Lower to Middle Jurassic of the southern High Atlas, Morocco. Ammonite and brachiopod fauna provide excellent biostratigraphic control on small scale stacking patterns.

At Amellago, the evolution of depositional environments is evident at different scales of space and time during this period of tectonic quiescence dominated by thermal subsidence. An important observation is that the Amellago ramp system contains micrite-rich, ooid-free intervals that alternate with ooid-rich intervals. The ooid-rich intervals are mainly in the late transgressive and highstand system tracts, whereas the ooid-free intervals occur in the early transgressive phase. More than 25 such alternations were recorded in high frequency cycles and at the scale of one large cycle at the Aalenian/Bajocian transition. These compositional changes and the associated different ramp geometries are interpreted to result from the combined effects of eustatic sea level and climatic changes.

Carbonate ramps display a wide spectrum of depositional profiles and facies belts (Burchette *et al.* 1990; Burchette & Wright 1992; Badenas & Aurell 2001). The distinctive character of carbonate ramp systems shows the control of the physical, chemical and biological conditions that result from variations in palaeoclimate, tectonic regime, ecological changes, etc. Ramp systems are an important component of many carbonate successions, particularly during the early stages of the platform evolution (Read 1985). Ramps are widespread throughout the geological record and were particularly common during Mississippian and Jurassic times (Burchette *et al.* 1990; Burchette & Wright 1992; Badenas & Aurell 2001). Ramp systems contain significant hydrocarbon reserves. In particular, oolitic ramp systems form important reservoirs in various sedimentary basins of which the Upper Jurassic Smackover Formation of the US Gulf Coast is one of the best known (Heydari 2003). Other such examples are the Middle and Upper Jurassic reservoirs of the Persian Gulf: Marrat, Dhruma, Izhara and Araej Formations (Alsharhan & Kendall 1986; Alsharhan & Whittle 1995).

Although the factors controlling carbonate production and accumulation are relatively well understood, the analysis of ancient carbonate rocks is commonly challenged by the complexities of stratigraphic packaging and by incomplete or poorly exposed outcrops. A good knowledge of reservoir architecture (geometries and reservoir facies dimensions) is paramount for the construction of geological models and geostatistically-based reservoir simulations (Lomando 1998; van Buchem *et al.* 2002).

Unfortunately, most of the models in literature (Aurell *et al.* 1995, 1998; Badenas & Aurell 2001; Burchette *et al.* 1990) are based on poorly exposed and/or discontinuous outcrops. This fragmentation compromises fine-scale observations where the precise facies geometries within high-frequency cycles need to be understood. This study presents the relationships between stratal and lithofacies anatomy in an almost completely exposed ooid-dominated ramp system in the Lower to Middle Jurassic. The outcrops are located at the southern flank of the High Atlas in Morocco and have seismic scale dimensions (35 km long and about

From: VAN BUCHEM, F. S. P., GERDES, K. D. & ESTEBAN, M. (eds) *Mesozoic and Cenozoic Carbonate Systems of the Mediterranean and the Middle East: Stratigraphic and Diagenetic Reference Models.*
Geological Society, London, Special Publications, **329**, 65–88.
DOI: 10.1144/SP329.4 0305-8719/10/$15.00

1000 m thick). A reliable biostratigraphic framework based on ammonites and brachiopods provides excellent time stratigraphic control on the scale of high frequency cycle (small scale) stacking patterns. This allows the analysis of the spatial distribution of oolitic facies and peloidal facies within high-frequency cycles as well as the evolution of depositional environments at different scales of time and space. The understanding of the controls on production and redistribution of ooids and pellets in oolitic ramp settings will help in predicting facies architecture in analogue reservoir rocks in the subsurface.

Geological setting

The study area is located on the southern flank of the Central High Atlas mountain belt, approximately 30 km north of Goulmima (Fig. 1a), on both sides of the Gheris Valley (Fig. 1b). Uplifted during Cenozoic times, this mountain area evolved from an intracontinental basin called the High Atlas Trough (Ellouz *et al.* 2003; Arboleya *et al.* 2004; El Harfi *et al.* 2006*a*, *b*). During early Mesozoic times, this trough was a corridor open to the Tethyan Ocean that developed at the boundary between the Saharan Craton and the Moroccan Mesetas (Fig. 1b).

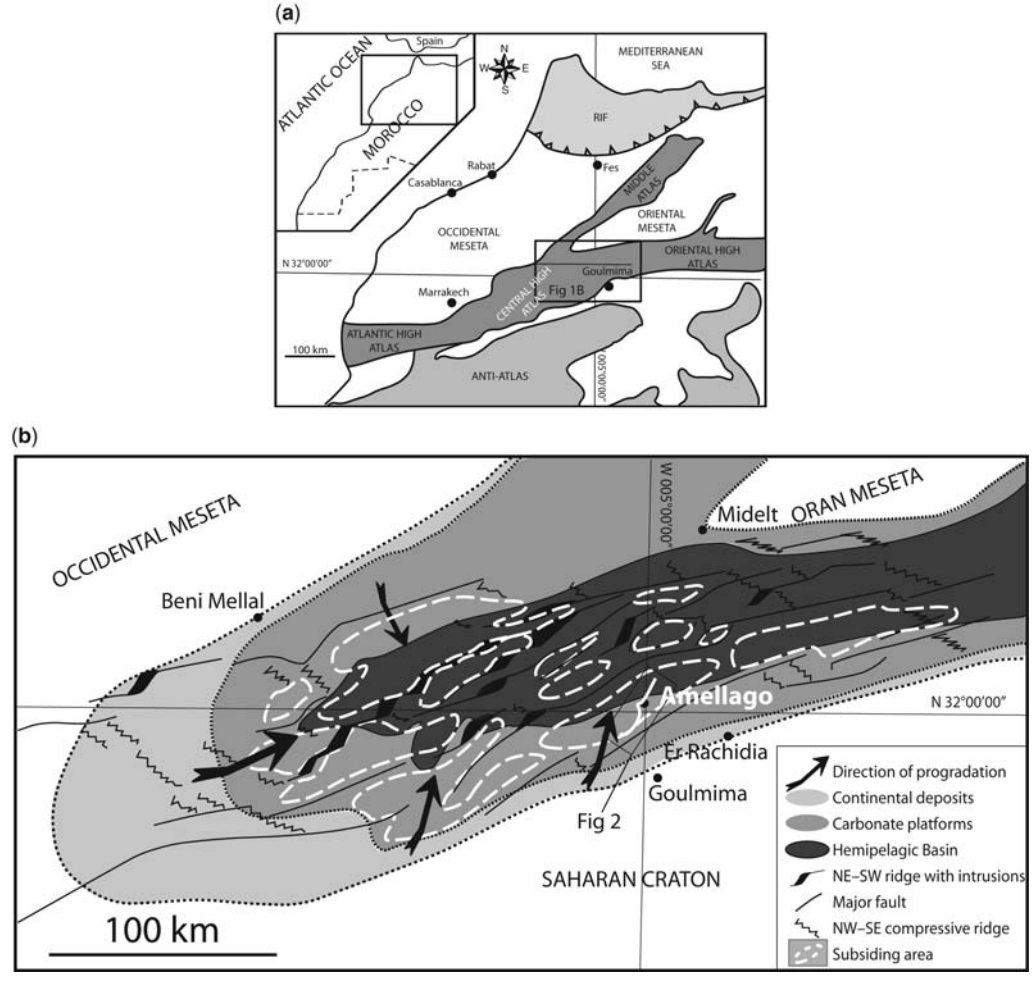

Fig. 1. (**a**) Map of the main structural domains of Morocco (modified after Pique & Michard 1989). The Rif is a mountainous arc that was thrust southward and dominates northern Morocco. The western and eastern Mesetas constitute individual microplates from Atlantic rifting. The Atlas thrust-belts extend 2000 km from the Atlantic Ocean to the Mediterranean in Algeria. The Anti-Atlas is the southernmost mountain belt of Morocco and is oriented ENE–WSW. (**b**) Tectonic and palaeogeographic diagram of the High Atlas basin during the Toarcian and location of the Amellago transect (compiled and modified from Laville 1985 and Milhi *et al.* 2002).

According to numerous studies, the basin evolution can be summarized into two main tectonically-induced sedimentary phases, both linked to the Western Tethys and Central Atlantic rifting-drifting processes that occurred during the same period (Mattauer *et al.* 1977; Laville 1981; Ait Brahim *et al.* 2002). The first phase took place during north–south to NW–SE extension in the late Triassic to the late Lias when a true rift basin, created by NE–SW syn-sedimentary extensional faults, appeared at the northern boundary of the Saharan Craton. During the Triassic, well-developed half grabens were filled with tholeitic basalts, fluvial sandstones, and continental red beds and evaporites (Michard 1976; Pique & Michard 1989). During the early and middle Lias, the rifting phase continued with a rapid increase in accommodation space. Block tilting caused by high strain normal faults (Sarih *et al.* 2007) led to a major marine incursion from the Tethys Ocean and to a well-developed hemipelagic depocentre bordered by carbonate platforms (Wilmsen & Neuweiler 2008). The carbonate platforms are characterized by bioconstructed shelf breaks and steeply-inclined slopes along the borders of the basin or on the tilted blocks. At the end of the rifting phase, during the lower and the middle Toarcian, a eustatic rise of sea level caused a major drowning of all the regional carbonate platforms (Pique 1994; Elmi *et al.* 1999; Wilmsen & Neuweiler 2008).

The second tectonosedimentary phase, that is, the post-rift evolution of the basin, began during the late Toarcian (upper Lias deposits), when the sinistral movement of Africa relative to Eurasia induced a transtensional regime. This led to the development of a mosaic of rhomb-shaped depocentres bounded by syn-sedimentary ridges (Laville 1988; Brede *et al.* 1992; Laville *et al.* 2004). From the late Toarcian to the late Bajocian, most of these depocentres were filled by hemipelagic marls, whereas carbonate platforms nucleated on the margins of the rhomb-shaped basins (e.g. the Amellago-Agoudim ramp system described here). In the late Bathonian or Callovian, the structural regime became transpressive and the High Atlas Trough was emergent.

The Amellago transect is a series of cliffs and steep hillsides that form a quasi-continuous section across the Lias–Dogger platform-basin system (Fig. 2). The transect is oriented SSW–NNE and cross cuts the southern margin of a rhomb-shaped basin that developed between two syn-sedimentary faults, the Foum Zabel fault to the south and the Tagountsa fault to the north (Fig. 2). This seismic scale outcrop allows direct tracking of the stratal geometry and the facies migration that occurred along the palaeoslope.

Two formations are well exposed in this transect (Figs 2 & 3). The Agoudim Formation (lower Toarcian to lower Bajocian) includes mainly blue and grey marls deposited in offshore environments (Hadri 1993). It forms the substratum, the cover, and the distal parts of the studied Amellago Formation (Fig. 3). The Amellago Formation includes all of the neritic carbonates that were deposited in the area from the late Toarcian to the early Bajocian. The Amellago Formation represents an oolitic carbonate ramp system that prograded northward into the subsiding basin (Figs 3 & 4) (Poisson *et al.* 1998; Durlet *et al.* 2001).

Methods

Nearly 50 sedimentological sections (6400 m of cumulative thickness) were described for facies analysis and to collect biostratigraphic information. More than 350 thin sections were analysed petrographically and, along with the field observations, formed the basis for eight facies associations with a total of 22 facies types (Table 1; Figs 5, 6 & 7). The 'depositional region' terminology was modified from Tucker & Wright (1990), who defined an inner ramp and outer ramp, respectively located landward and seaward of the ooid shoal, which represents the middle ramp setting. Classically, the hemipelagic basin corresponds to the lower offshore zone deposits (Table 1). This terminology is well suited to the broad-scale progressive lithological changes that we observed between different environments along low-angle chronostratigraphic surfaces of the 2D strata framework.

Measured sections were correlated by tracking high frequency sequences from inner ramp to basinal environments. Observations were recorded on photo mosaics including photos taken from the air in a microlight aircraft. Such photos have a resolution of about 10–20 cm and were generally orientated perpendicular to the actual (dip direction) cliff face, instead of oblique from the foot of the cliff. Three high resolution cycles were selected for a detailed study because of their continuity and their accessibility in the field. The three cycles, each 20 to 30 m thick, have been traced in the field from the proximal to the most distal areas. Such correlations form the basis for the structural framework, the spatial and temporal facies relationships, the regional stratigraphic framework and the different facies models.

Facies description

The facies are grouped in five main depositional environments comprising different sets of facies associations.

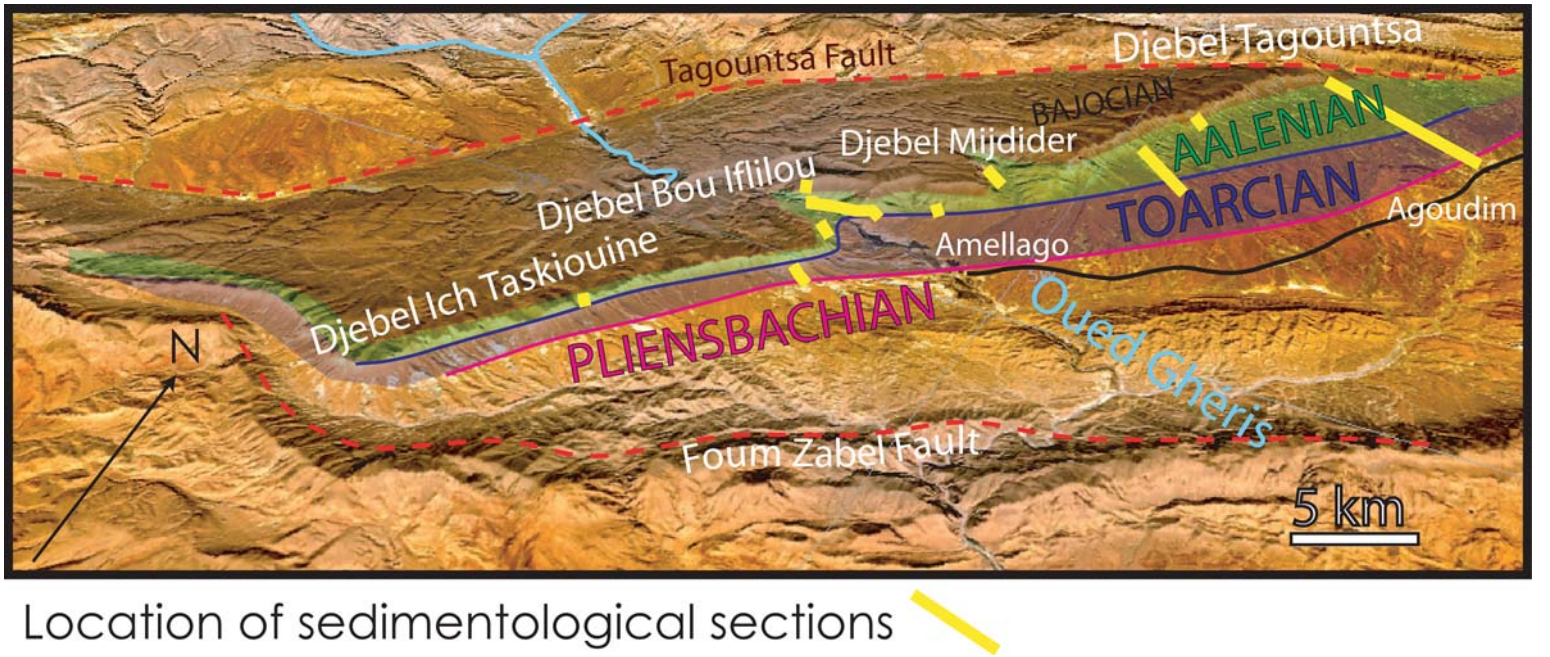

Fig. 2. 3D view of Amellago transect showing the sedimentological series ages, the main sections and main geographic features (from Worldwind).

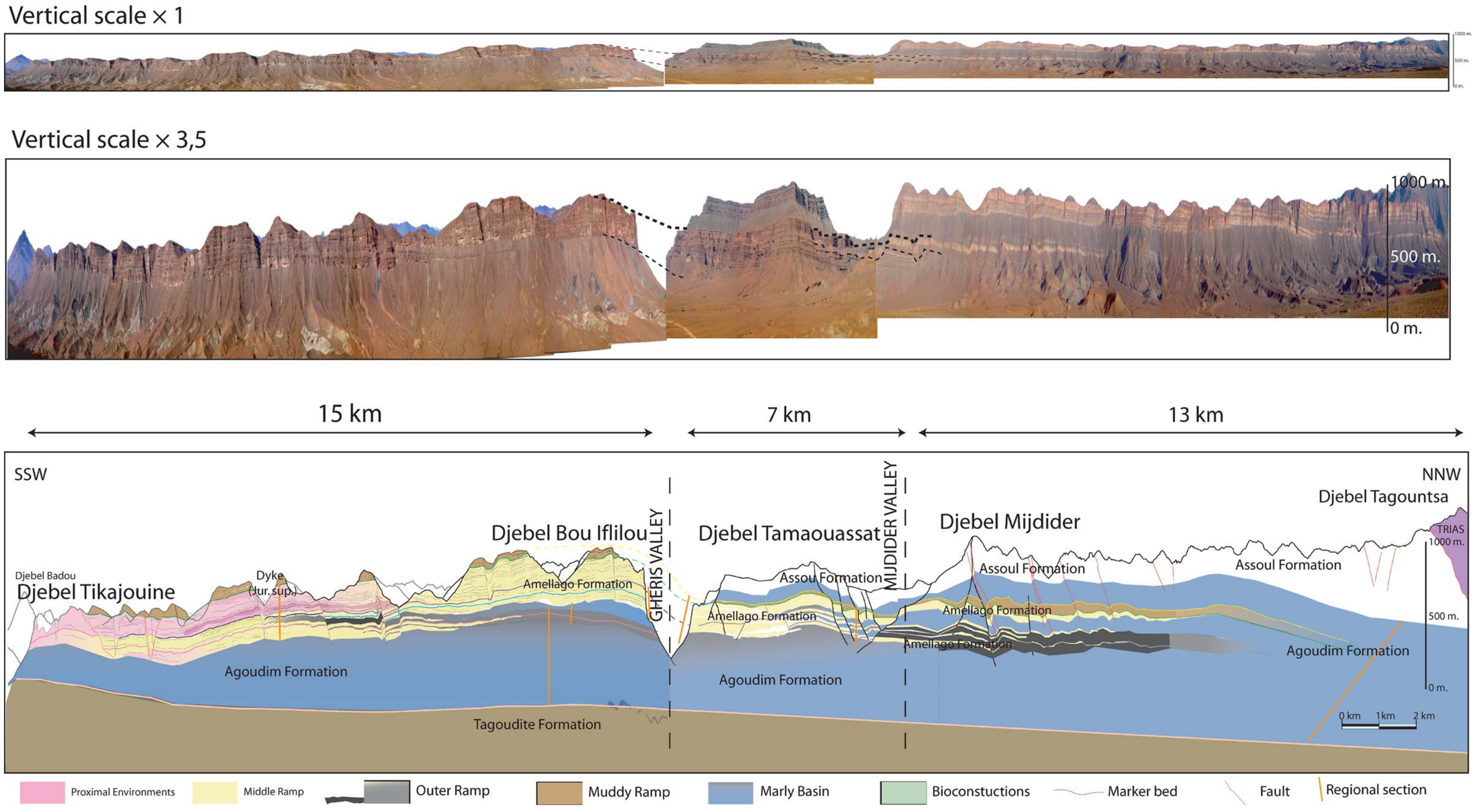

Fig. 3. Photo-montage of the Amellago transect with the formations and members interpreted in terms of major depositional environments. Vertical scale (×3.5) is exaggerated because of the very flat ramp geometries.

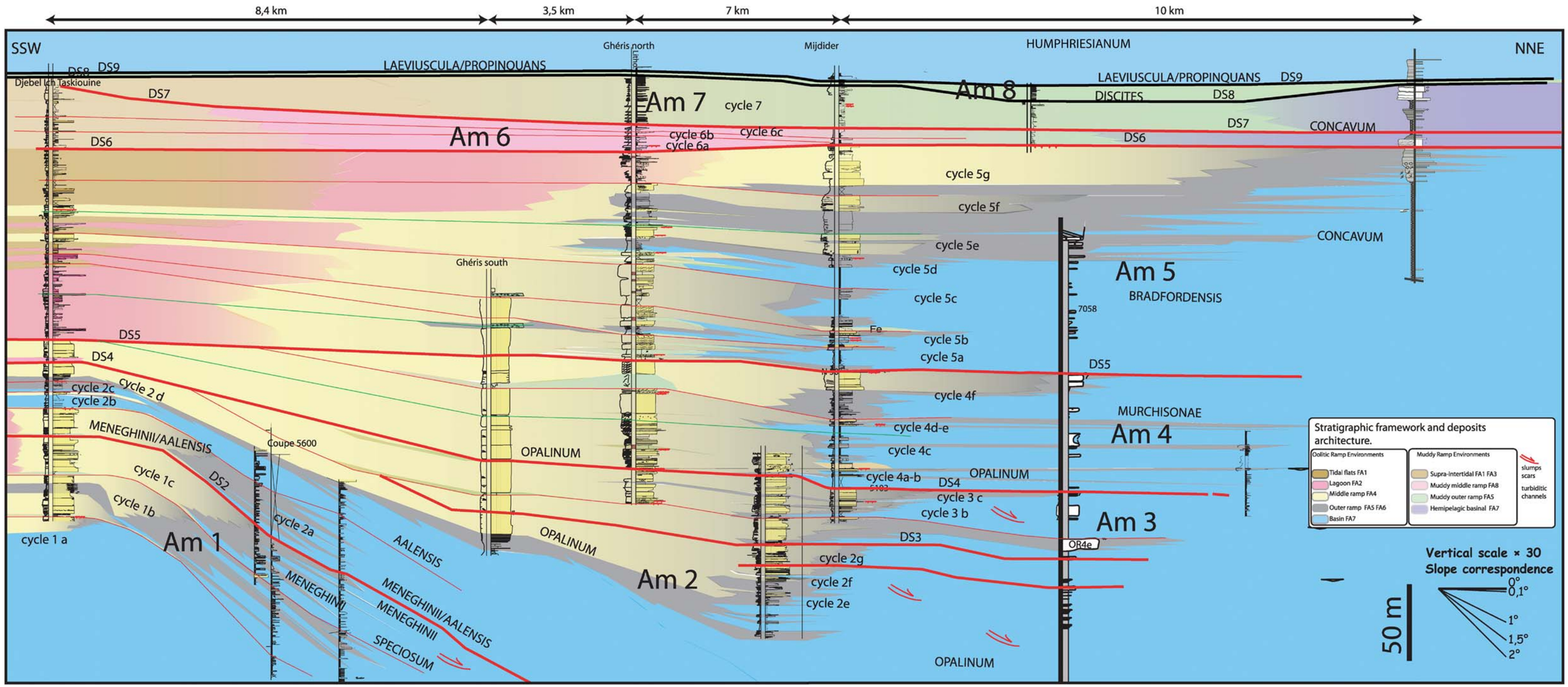

Fig. 4. Stratigraphic correlation at the third-order scale from upper Toarcian to lower Bajocian. Am2 to Am5: aggrading-prograding Oolitic Ramp Sequences. The sequence Am2 is the first occurrence of a shallow carbonate platform in the area since the Pliensbachian. At the Djebel Ich Taskiouine measured section, sequence Am2 reaches 70 m of thickness. The oobioclastic facies (FA5) belt attains 8–10 km of proximal-distal extension. At a smaller time scale, two high frequency cycles can be easily differentiated within Am2, both on pictures and on sedimentological sections. Sequences Am3 and Am4 show multiple toplap geometries, observed on the microlight pictures (see Fig. 8). Cumulative thickness of these sequences is 30 m on Djebel Ich Taskiouine but reaches more than 250 m northward, near Ksar Agoudim. Such thickness variation indicates that during this period, the northern part of transect was clearly subsiding more than the southern part. Elmi (1990) and Sadki (1992) already reported margin uplifts and basin subsidence. Oobioclastic facies (FA 4) are volumetrically dominant in sequences Am3 and Am4, which both show the farthest progradation. The resulting oobioclastic facies belt reaches a width of 20 km at the maximum of progradation. Sequence Am5 is a complete transgressive-regressive cycle. The prograding phase is accompanied by the development of oolitic grainstone facies (FA 4), which forms low angle clinoforms during this third-order highstand. The average extent of oolitic facies belts (shallow ramp facies) reaches 15 km during prograding phases and 8 km during retreating phases. Sequences Am6, Am7 and Am8: aggrading-retrograding muddy ramp sequences end the deposition of Amellago Formation during the Bajocian.

Table 1. *Facies classification. The last last three columns display the main characteristics of the 22 lithofacies in terms of sedimentary structures and main Dunham (1962) textures*

Environment	Facies association and bathymetry	Facies ('litho-facies') Code	Name	Structure and energy	Main content
Inner ramp	FA1 Supratidal to intertidal	F1a	Tidal flats marls	Laminated	Micrite, illite, chlorite, quartz and feldspar
	+2 to −2 m	F1b	Mudflat M	Laminated, mudcracks, microbial crusts	Micrite, benthic foraminifera
		F1c	Grainy tidal flats W-P	Fenestral, mud cracks	Pelloids
		F1d	Restricted marine dolomicrite	Laminated with sulphate pseudomorphs	Dolomicrite, sulphates
	FA2 Lagoon	F2a	Lagoon marls	Laminated, low energy	Gastropods
	0 to −3 m	F2b	Lagoonal micritic limestone W-F	Massive, low energy	Large oncolites
		F2c	Lagoonal grain-dominated limestone P-G	Massive to laminated, moderate energy	Pelloids, aggregates
		F2d	Storm wash over and tidal inlet P-G	2D megaripples and cross beds, high energy	Ooids
	FA3 'Open' muddy lagoon	F3a	Coarsening-up M to G with mudclasts	Massive to laminated, burrows	Pellets, mudclasts, bivalve and coral clasts
	0 to −10 m	F3b	Marls	Laminated	Brachiopods
Middle ramp	FA4 Oolitic belt	F4a	Tide influenced shoal G-P	Tidal structures (e.g. sigmoids, climbing ripples, channels, bi-directional cross-bedding)	Pellets, ooids, bioclasts
	0 to −10 m	F4b	Wave influenced shoal G	2D and 3D megaripples	Ooids, bioclasts
		F4c	Coarse-grained shoal R-G	Massive and 2D megaripples	Corals and shells fragments
Outer ramp	FA5 Upper offshore type 1	F5a	Toe of shoal fine grainstone	2D ripples to massive, bioturbated	Fine pellets, ooids, bioclasts
	−10 to −35 m	F5b	Proximal tempestites R-G-P-W-M	Erosive base, scours, HCS	Pellets, ooids, bioclasts
		F5c	Nodular W-P	Wavy, massive to laminated	Pellets, ooids, bioclasts
		F5d	Patchy coral bioconstruction B	Massive	Corals, bivalves, brachiopods, echinoderms

(*Continued*)

Table 1. *Continued*

Environment	Facies association and bathymetry	Facies ('litho-facies') Code	Name	Structure and energy	Main content
	FA6 Upper offshore type 2 −20 to −50 m	F6a	Heterolitic wavy beds W-P	Nodular, *Thalassinoides*	Large bivalves (*trichites, pholadomia* and *tridacnea*)
		F6b	Distal tempestites R-G-P-W-M	Erosive base, HCS normally graded beds (rudstone to mudstone with marls)	Pellets, ooids, bioclasts
		F6c	Biostrome B	Stratified	Corals, bivalves, brachiopods, echinoderms
Basin	FA7 Hemipelagic basin −35 m to −150 m ?	F7	Lower offshore to basin marls	Planar laminar, some slumps, low energy	Rare ammonites, belemnites, zoophycos
Ooid-free muddy ramp	FA8 −10 m to −35 m	F8	Glauconitic peloidal sand P	Heavily bioturbated, some scours and HCS, generally low energy	Foraminifera, pellets, micritic intraclasts, brachiopods, bioclasts, detritic quartz, wood debris

HCS, hummocky cross-stratification; M, mudstone; W, wackestone; P, packstone; G, grainstone; R, rudstone; F, floatstone; B, boundstone.

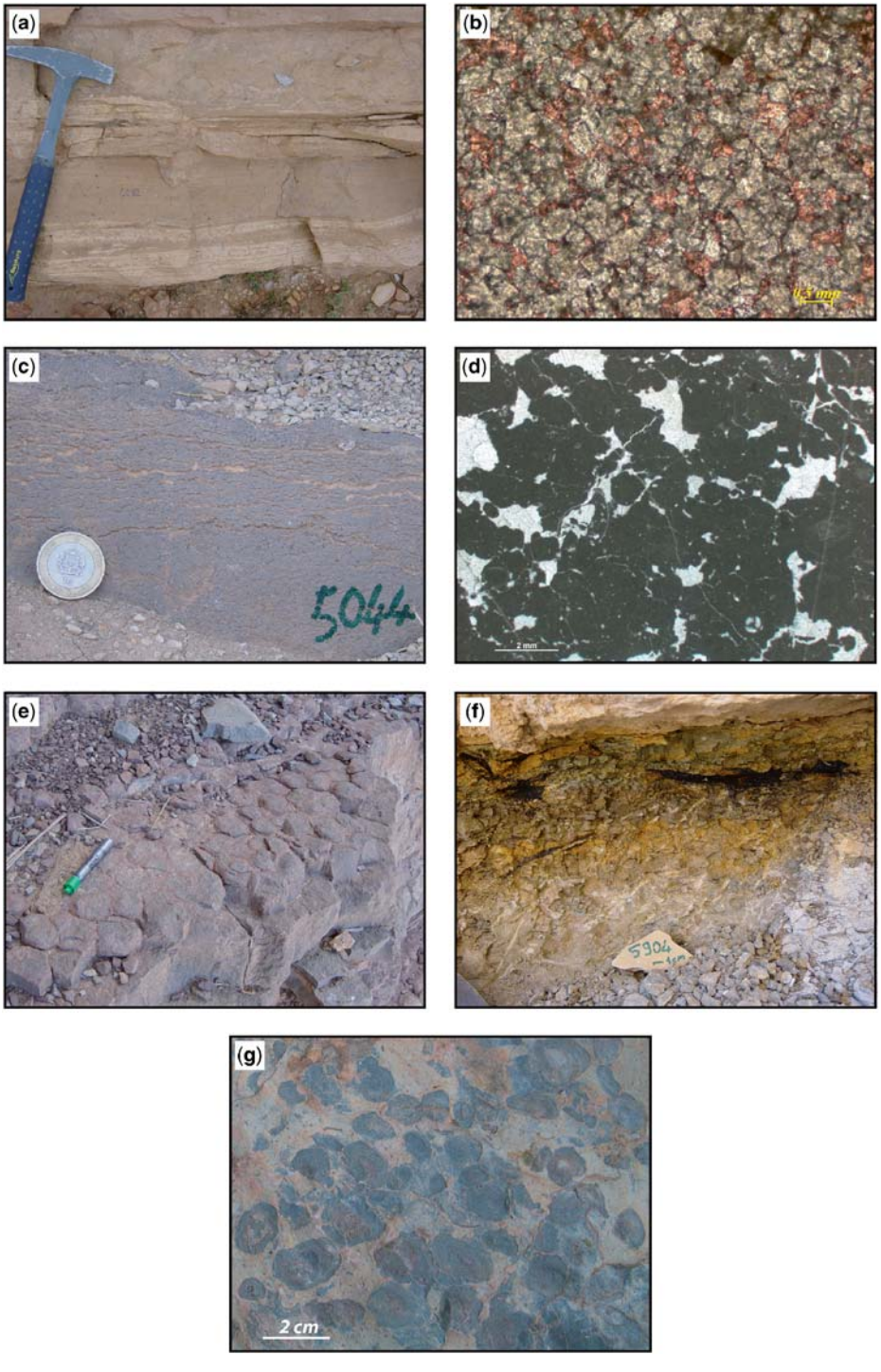

Fig. 5. Inner ramp facies belt pictures. (**a**), Facies 1b, laminated mudstone with rip-up clasts; (**b**), Facies 1d, anhedral to subhedral dolomite anhedral, inclusion rich; (**c**), Facies 1c, fenestral texture, outcrop; (**d**), Facies 1c, fenestral texture, thin section; (**e**), Facies 1c, peloidal wackestone bed with mudcracks; (**f**), Facies 1a, coal debris (10–20 cm) within marls; (**g**), Facies 2b, floatstone with oncoids.

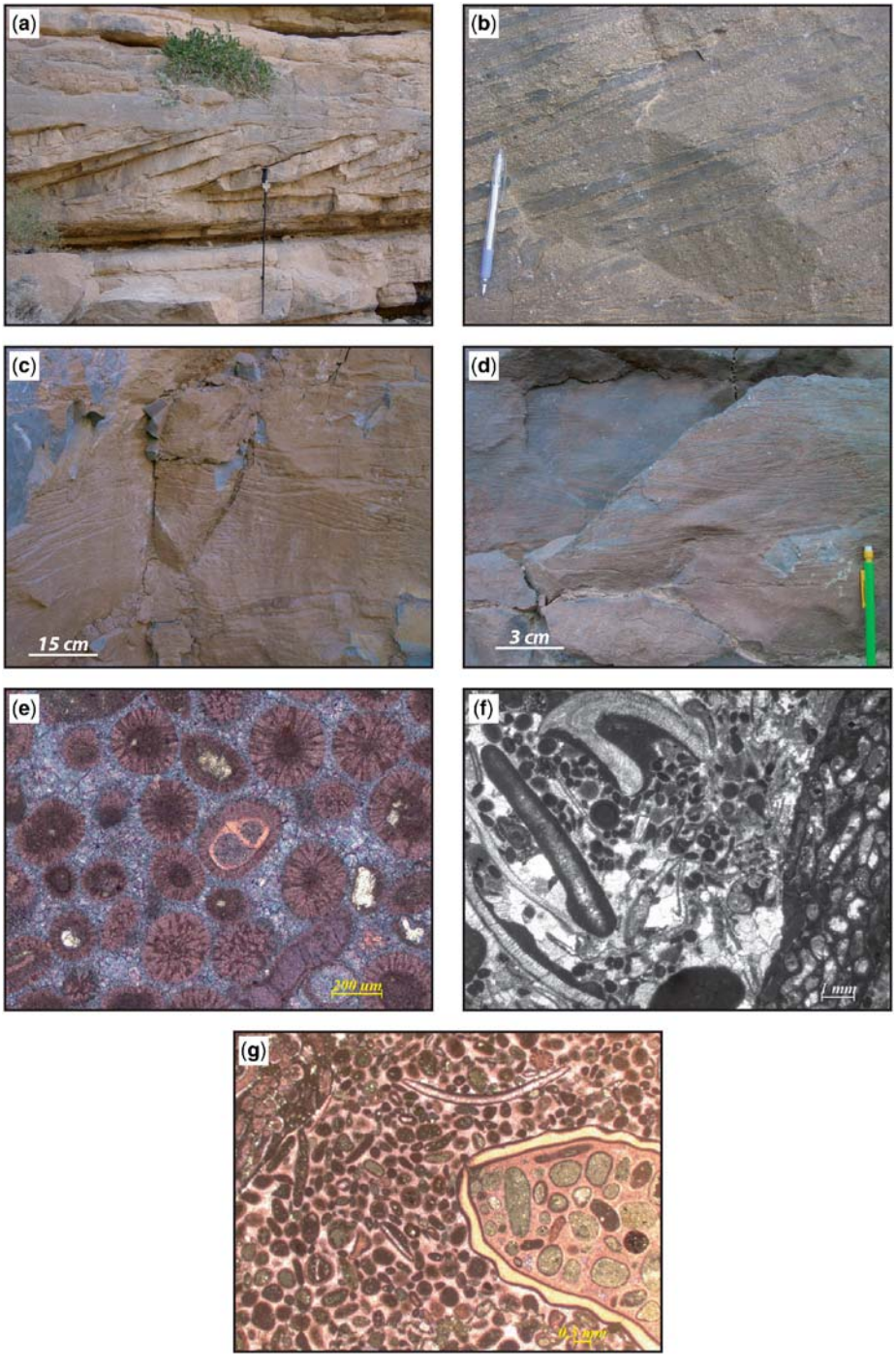

Fig. 6. Middle ramp facies belt pictures. (**a**), Facies 4a, tide-influenced shoal (note the size and the cyclicity of bundles; Jacob's staff = 1.5 m); (**b**), Facies 4a, tide-influenced shoal with composite stratification, decantation lamination and subordinate ripples; (**c**), Facies 4b, tabular cross-bedded oobioclastic grainstone; (**d**), Facies 4b, trough cross-bedded oobioclastic grainstone; (**e**), Facies 4b, grainstone detail with radial-fibrous ooids; (**f**), Facies 4c, grainstone with ooids, peloids and bioclasts; (**g**), Facies 4a, grainstone with superficial ooids, bivalve fragments and serpulids.

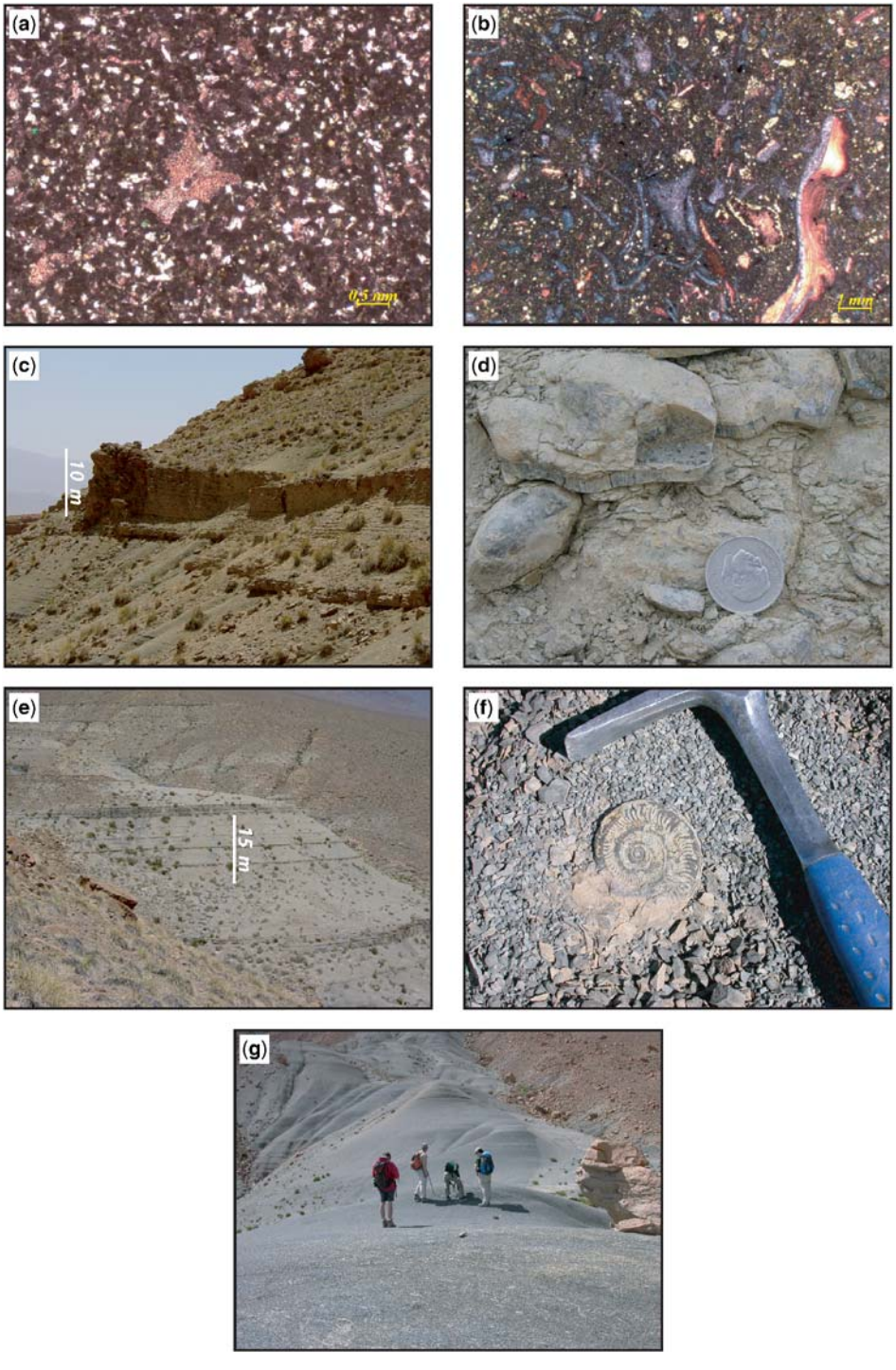

Fig. 7. Outer ramp facies belt and basin pictures. (**a**), Facies 8, very fine packstone with peloids, echinoid fragments, dolomite, glauconite and quartz; (**b**), Facies 5c, wackestone with various bioclasts; (**c**), Facies 6c, bioconstruction at the offshore-basin transition; (**d**), Facies 6a, trichites and terebratula in life position; (**e**), Facies 6a and 7 alternations; (**f**), Facies 7, *Hildoceras bifrons* (ammonites); (**g**), Facies 7, hemipelagic marls.

Inner ramp

The inner ramp is located immediately landward of the ooid shoal belt and was a low-energy protected setting. The facies associations are dominated by micritic limestone, dolomicrite and marls which generally indicate low- to moderate-energy subtidal, intertidal and supratidal settings (Table 1 and Fig. 5).

Facies Association 1: supratidal to intertidal environment. This facies association occurs in four intervals and is characterized by decimetre scale, tabular shaped beds with abundant ostracods, benthic foraminifera and gastropods.

- *Facies 1a: tidal flat marls*: composed of red to green marls containing illite, chlorite, quartz, and feldspar.
- *Facies 1b: mudflat*: consists of laminated mudstone with generally well-preserved mudcracks near the top of the intervals and locally contains rip-up clasts.
- *Facies 1c: grainy tidal flat*: is dominated by peloidal grainstone to wackestone with peloids 0.25 and 4.0 mm in diameter. Fenestral fabrics and polygonal mud cracks are also common. They are indicative of sub-aerial exposure.
- *Facies 1d: restricted marine*: is dominated by Fe-poor and inclusion-rich dolomite. The dolomite usually forms small euhedral crystals but large inclusion-free overgrowths may also occur. The paragenetic relationships indicate that dolomite precipitated prior to all other diagenetic phases. Small calcitic nodules that are 1 cm to 4 cm in diameter may occur within dolomite beds. Their occurrence between laminated dolomitic crusts, their shape, and their association with collapse breccias are indicative of ancient evaporite nodules that have been calcified. For all these reasons, the facies 1d dolomite is thought to have been deposited in a restricted marine environment (intertidal to supratidal), with intermittent phases of evaporation.

Facies association 2: lagoon environment. The subtidal lagoon facies association occurs in three intervals of decimetre to metre scale and tabular bedding.

- *Facies 2a: lagoonal marls*: is composed of marls containing very rare fauna (gastropods).
- *Facies 2b: lagoonal micritic limestone*: consists of oncoidal wackestone to floatstone containing large micritic spheres with irregular cortices interpreted as oncoids (8 mm average diameter up to 2 cm). Vertical and horizontal burrow systems interpreted as *Thallasinoides*, probably of crustacean origin, are very common.
- *Facies 2c: lagoonal grain-dominated limestone*: is composed of peloidal packstone to grainstone with abundant well-sorted and well-rounded peloids and rare ooids. There are two types of peloids: faecal pellets and mud lithoclasts and their origin is often hard to determine. In some cases, the uniformity of their sizes and shapes is a clue that they are of faecal origin. Sometimes, peloids form aggregates with soft (deformed) intergranular contacts. The preservation and the burial of pellets are possible in this low energy environment. Also common are gastropods and vertical and horizontal burrows (*Thallasinoides)*.
- *Facies 2d: storm washover lobes and tidal inlet grainstone*: is characterized by coated-grain grainstones with a small proportion of bioclasts. It occurs in up to 1 m thick, 2D megaripple cross-beds that migrate landward (southward) and pinch out within facies 2a, 2b and 2c. The oobioclastic mega-ripples also form lenses detached from the oolitic shoal. The grainy beds are attributed to high-energy events and depositional sub-environments of storm washover lobes and tidal inlets that are located in an otherwise protected shallow marine environment behind the oolitic shoal.

Facies association 3: open-marine muddy ramp environment. The subtidal, open-marine, muddy ramp association occurs in three decimetre to metre thick, tabular bedded intervals.

- *Facies 3a: mudstone to mudclast grainstone in graded beds*: consists of beds with a mudstone base transitioning upward into wackestone with mudclasts followed successively by coarse, mudclast packstone and then mudclast grainstone. The bed tops are commonly bioturbated, bored, and iron stained. The mudclasts in the wackestone are somewhat deformed possibly by compaction during very early stages of burial. In addition to mudclasts, rare shell fragments of brachiopods and bivalves and even more rare coral fragments are observed.
- *Facies 3b: open-marine, muddy ramp marls*: consists of marl deposits commonly associated with well-preserved brachiopods, which are indicative of low energy environments. The higher abundance of carbonate mud compared with the lagoon and the absence of a barrier or any oolitic shoal justifies the interpretation as an open-marine environment.

Middle ramp

The shallow ramp area is dominated by oobioclastic grainstone (Facies association 4, Table 1; Fig. 6). When homogeneous shallow ramp grainstone facies of several high-resolution cycles are stacked, they constitute the most impressive cliffs of the Amellago transect (up to 200 m thick).

Facies association 4: oolitic belt environment. Facies association 4: Oolitic belt: consists of three decimetre to metre scale, alternating, mainly tabular but also lobe-shaped facies bodies. Based on sedimentary structures, three facies types are distinguished.

- *Facies 4a: tidal influenced shoal*: is characterized by bi-directional cross-beds, alternations of fine and coarse bedsets showing a cyclic organization, and sigmoidal cross stratification typical of tidal environments. Facies 4a is interpreted as tidal oolitic sand bars in a tidal inlet.
- *Facies 4b: wave influenced shoal*: is mainly composed of grainstone and exhibits 2D and 3D mega-ripple cross beds and low angle cross beds that appear to prograde seaward. Reactivation surfaces are present. The deposits are organized along low angle (up to 3–4°) clinoforms, which also show a seaward migration. Facies 4b is interpreted as shoreface sands.
- *Facies 4c: coarse shoal facies*: consists of massive deposits of coarser bioclastic debris (molluscs, echinoderms, and corals).

In general, Facies association 4 is dominated by oobioclastic grainstones with subordinate packstones. Grainstones are composed of ooids and bioclasts with 70% of non-skeletal grains.

Three types of ooids can be differentiated based on thin-section analysis: (1) radial-fibrous ooids with several regular cortical layers; (2) superficial ooids with a thin cortical layer; and (3) small micritic ooids (Fig. 6). Nuclei of radial-fibrous ooids and superficial ooids are mostly peloids, but can also be bioclasts, aggregate grains and lithoclasts. There are also composite ooids in which the nucleus consists of one or several ooids held together by a micritic matrix. Ooid cortices have a radial crystal structure interrupted by thin, dark micritic layers. Some peloids that form nuclei are dolomitized and stained red by iron oxides, facilitating identification with a hand lens. Bioclasts (echinoderms, bivalves, brachiopods, gastropods, bryozoans and foraminifera), lithoclasts and aggregate grains are quite common within the grainstones. Sorting and concentration of the different components depends on the position within a high-resolution cycle. The described sedimentary structures and grain-rich nature of this facies association indicate deposition on a high-energy, ooid shoal under the influence of fair weather waves and local tides.

Outer ramp

Facies association 5: proximal upper offshore environment. Facies association 5 contains four different facies types with variable stratigraphic organization.

- *Facies 5a: toe-of-shoal fine grainstone*: is dominated by very fine to fine, well-sorted, and well-rounded peloidal grainstone to packstone. The abundant peloids with an average diameter between 0.20 and 0.5 mm have a distinctive round shape. Their regular size, shape and internal concentric structure suggest a faecal origin. Other common allochems are ooids and bioclasts. Sedimentary structures such as ripples are often destroyed by intense bioturbation, which suggests that sedimentation rates were probably reduced and the environment was at least intermittently subject to low-energy conditions.
- *Facies 5b: proximal tempestites*: consist of fining upward, decimetre-scale, lensoidal beds (rudstone to mudstone) that are 10 to 70 cm thick. The beds are commonly amalgamated with erosive bases and usually show hummocky cross stratification (HCS) in the proximal part. These beds are interpreted as tempestites in the sense of Aigner (1985) and deposited between fair weather wave base (FWWB) and storm wave base (SWB). Graded beds interfinger with bioturbated limestone and marls just below the SWB in the distal part.
- *Facies 5c: nodular wackestone packstone*: is composed of peloids and bioclasts (brachiopods, bivalves and echinoderms fragments). In distal areas, coquinas are found scattered or concentrated in pockets and are associated with erosive features with normally graded bioclasts and/or HCS. These deposits are interpreted as tempestite relicts that were reworked by bioturbation. The depositional environment is interpreted as a weakly agitated area from distal shoreface to proximal offshore.
- *Facies 5d: coral bioconstructions*: is composed of framestone to bafflestone and occurs in patches of about 5–10 m width and 1–2.5 m height. Hermatypic corals with mainly branching and domal forms and sponges form the framework of the buildups. Corals are rarely reworked indicating deposition below the FWWB. Buildups formed within tempestite deposits and are interpreted to occur in the photic zone in the proximal part of the offshore environment.

Facies association 6: distal upper offshore environment. The offshore facies association type 6 (distal) consists of 3 different facies types with various natures and various origins.

- *Facies 6a: heterolithic wavy beds*: is composed of alternations of tabular 2–5 cm thick beds of marls and 2–10 cm thick beds of mudstone to wackestone. *Thalassinoides* traces attest that the nodularity probably results from the combination of heterogeneous bioturbation and

compaction. The presence of large bivalves (*trichites, pholadomia* and *tridacnea*) usually in life position attests to an open-marine, distal depositional environment.

- *Facies 6b: distal tempestites*: consists of normally graded beds (rudstone to mudstone) of 10–70 cm thickness. This facies is similar to Facies 5b with the exception that the tempestites beds are interbedded with thin layers of marl. The lower limit of the deep ramp is marked by the disappearance of the graded tempestite beds.
- *Facies 6c: stratified bioconstructions*: is characterized by columnar-shaped facies bodies with average dimensions of 3 m width by 6 m thickness. In exceptional cases, biostromes of 100 m width and 20 m thickness were observed. The bioconstructions are composed of hermatypic corals of various forms, sponges, and large bivalves (*tridacnae*) that are slightly broken up. These carbonate masses are formed by successive layers slightly thickened (few decimetres) that differ from surrounding Facies 6a rocks. Relationships with surrounding layers show that: (1) their palaeo-elevation was low, on the order of several decimetres above the seafloor; and (2) they grew in the distal part of the upper offshore zone and formed in water depths of a few tens of metres.

Hemipelagic basin

Facies association 7: Lower offshore to basin environment. Facies association 7 is represented by one homogeneous facies.

- *Facies 7: Lower offshore to basinal blue-grey marls*: is composed of blue-grey marls with an average carbonate content of 20–30%. Others components are clays (illite, chlorite) and fine terrigenous grains (quartz and feldspars). The fauna are mainly composed of ammonites, small bivalves and small gastropods.

Ooid-free muddy ramp

Facies association 8: Inner to mid ramp environment. Facies association 8 is represented by one facies. It forms homogeneous argillaceous microwackestone to micro-packstone prisms that are several kilometres in extent and with a thickness of several decimetres to a metre.

- *Facies 8: glauconitic peloidal packstone*: is composed dominantly of small peloids and accompanied by common glauconitic and quartz grains, wood debris, and microbored bioclasts including bryozoans, foraminifera, brachiopods, gastropods, and bivalves. Radial-fibrous ooids and micritic ooids are never present, whereas superficial ooids and ooid fragments are very rare. This facies is often dolomitized, especially in the proximal parts of the prisms. The beds are structureless, which is interpreted as a sign of intense bioturbation. The weathering gives a light beige colour to this ooid-free enigmatic facies (see part 5).

Evolution of the ramp system at the large scale

Stratigraphic architecture

The migration of the facies belts seaward (progradation) and landward (retrogradation) are easily identifiable in the Amellago transect. On the basis of their internal progradational, aggradational and retrogradational geometries (Fig. 3), the Agoudim and Amellago Formations can be subdivided into a hierarchy of three orders of cycles, large, medium and small (Durlet et al. 2001) (Table 2).

Table 2. *Biostratigraphic zones for stratigraphic surfaces with numerical ages from Gradstein* et al. *(2004)*

Surfaces and medium scale cycles	Ammonites biozones from Groupe Français d'etude du Jurassique (1999)	Calculated numerical ages for stages boundaries from Gradstein *et al*. (2004)	Stages
DS9	Discites/Laeviuscula/ Propinquans		BAJOCIAN
		171.6	base BAJOCIAN
DS8–Am8	Concavum/Discites		AALENIAN
DS7–Am7	Concavum		AALENIAN
DS6–Am6	Concavum		AALENIAN
DS5–Am5	Murchisonae/Bradfordensis		AALENIAN
DS4–Am4	Opalinum (Bifidatum)		AALENIAN
DS3–Am3	Opalinum		AALENIAN
		175.6	base AALENIAN
DS2–Am2	Meneghini/Aalensis		TOARCIAN

Large-scale cycle. There is only one large-scale cycle (Fig. 4). The older (first) hemicycle starts within the thick deposition of several hundred metres of hemipelagic marls (Agoudim Formation) and finishes at the maximum basinward migration of the Amellago formation dominated by oolitic facies (FA4). The following hemicycle (second) is characterized by the landward migration of the Amellago Formation without any FA4 facies. Deposits from the retrograding and aggrading mud-dominated depositional systems lie on top of the oobioclastic ramp deposits.

Medium-scale cycles. At a higher frequency (medium-scale cycles have a thickness 50–100 m), five cycles of migration of facies belts seaward and landward along a dip section have been identified in the first large hemicycle (Am1 to Am5; Fig. 4). The surfaces at the bases of these cycles are noted as DS1 to DS5. Three medium-scale cycles are identified in the second large hemicycle (Am6 to Am8). The surfaces at the bases of these cycles are noted as DS6 to DS8. The top of Am8 is called DS9.

Cycles Am1 to Am5 each contain oolitic facies (FA4). Subsequently, an abrupt change in facies occurs near the Aalenian–Bajocian boundary, at the base of sequence Am6 (DS6). Above the DS6 surface, the successive environmental belts from the proximal to the distal ramp are represented by facies associations FA1, FA3, FA8, FA5 and FA7. The sedimentary system was a ramp with ubiquitous muddy textures but without ooids along the proximal distal transect.

Small-scale cycles. The five medium-scale cycles of the oldest large-scale hemicycle can be subdivided into 26 small-scale cycles (10–30 m thick; Fig. 4). Each small-scale cycle is bounded at its base by a discontinuity surface showing similar lateral sedimentological and diagenetic variations which will be described in 'Spatial and temporal distribution of facies within high frequency cycles' section.

In the youngest large-scale hemicycle, the medium-scale cycle 6 contains three small-scale cycles. The small cycles within medium-scale cycles 7 and 8 are difficult to observe and are not discussed in this paper.

Biostratigraphy and dating

The geological period studied here, from Toarcian and to Bajocian, is well dated by an abundant, diverse ammonite and brachiopod fauna (Durlet *et al.* 2001; Almeras *et al.* 2006; Pierre 2006; Bourillot *et al.* 2008). Correlations between measured sections as well as the timing of significant stratal surfaces are constrained by biochronological charts (Groupe Français d'Etude du Jurassique 1997; Almeras *et al.* 2006). The numerical ages of these timelines are calibrated to the timescale of Gradstein *et al.* (2004).

The ages of the medium-scale cycles are, respectively: Menegheni/Aalensis zones (late Toarcian) for Am1, Opalinum zone (Aalenian) for Am2 and Am3; Murchisonae zone (Aalenian) for Am4, Concavum zone for Am5 and Discites/Laeviuscula/Propinquans zones for Am6, Concavum zone for DS7, Concavum/Discites for DS8, and Discites/Laeviuscula/Propinquans for DS9 (Durlet *et al.* 2001; Pierre 2006).

Sequence stratigraphic and cyclostratigraphic interpretation

The sequence or cyclostratigraphic interpretation of the Amellago/Agoudim ramp system is based on the organization of the migration of facies belts landward or seaward along a dip section. The cycle or sequence definition is based on the notion of geological time. They are the result of tectonic, tectono-eustatic or glacio-eustatic mechanisms (Vail *et al.* 1991). The evolution of ramp system follows this hierarchy of cycles (large, medium and small).

The large-scale hemicycles are several hundred metres in thickness and record deposition over several millions of years (Ma) (Table 2; Fig. 4). They are considered second-order sequences (Vail *et al.* 1991). The first hemicycle is defined by the aggradation of Lower Toarcian hemipelagic marls (Agoudim Formation) and the northward progradation of the Amellago Formation dominated by oobioclastic ramps systems from the Toarcian–Aalenian transition, during the entire Aalenian and approximately to the Aalenian–Bajocian boundary (Sequences Am1 to Am5). The second hemicycle is defined by the southward aggradation–retrogradation of the Amellago Formation southward from the Aalenian–Bajocian transition to the middle Bajocian (Sequences Am6 to Am9).

The medium-scale cycles have an average thickness of 50–100 m (Fig. 4) and represent an average duration of 0.5–3 Ma. (Table 2). The updip and downdip shifts in facies zones (landward and seaward respectively) suggest the alternation of transgressive-regressive cycles (Fig. 4). They are considered third-order sequences (*sensu* Vail *et al.* 1991).

A high frequency cycle is defined as a composite transgressive-regressive interval bounded by two successive time surfaces of the same origin (Homewood *et al.* 1992). Thus, the small-scale cycles are considered high-frequency cycles (Fig. 4).

Spatial and temporal distribution of facies within high frequency cycles

Description of cycle architecture

This adopted methodology allowed the documentation of the lateral distribution of facies and discontinuities and their time relationships within three high-frequency cycles (Am2a, Am4a and Am4b) (Figs 8 & 9). The evolution of the depositional model along timelines within each high frequency cycle is described below.

Basal discontinuity surface. The basal discontinuity surface has been physically correlated and tracked. In the inner ramp environments, the surface is generally represented by a hardground that usually overlies and truncates the intertidal-supratidal dolomitic facies of the preceding high frequency cycle. The hardground forms a surface with irregular relief, local encrusting fauna and bivalve borings. Early cementation is indicated by micrite cementation and by thin isopachous calcite cements around allochems. This cement is inclusion-rich and shows a cloudy luminescence which suggests a high magnesium calcite (HMC) precursor (Moore 2001). It was probably precipitated from seawater in a phreatic environment during the sedimentary gap associated with the unconformity. Neither vadose and/or meteoric cements nor karstic or pedogenetic structures have been observed below or above this basal discontinuity surface.

In the mid-ramp, the surface is a planar hardground with numerous borings attributed to bivalves, echinoids and annelids. Iron hydroxides and encrusting fauna (oysters, bryozoans, and serpulids) are also present. Its lateral extent, from proximal to distal areas, reached more than 10 km with an average slope of 0.1–0.02°. Early lithification of the underlying oolitic grainstone is shown by the presence of isopachous fibrous cements, which are truncated by borings and by the planar surface itself. These calcitic cements are inclusion-rich and exhibit a cloudy luminescence indicative of HMC precursor cement. As shown in other studies (Dravis 1979; Loreau & Durlet 1999; Moore 2001), these characteristics suggest marine cementation and abrasion in an agitated shoreface environment. In this mid-ramp setting, the surface is covered by glauconitic calcisiltite FA8 or by hemipelagic marls FA9 in sharp contrast with the underlying oolitic grainstone. Basinward, the planar hardground shifts gradually to a bioturbated and non-lithified surface, and dissipates into an inconspicuous, conformable bedding surface within the hemipelagic marls of the basin.

Ooid-free interval. In this interval, the physical correlation of stratigraphic beds shows a depositional profile that is planar and slightly inclined (0.1–0.02°) without any slope break (Fig. 8). The entire ramp profile is dominated by muddy, peloidal and dolomitized lithofacies, and ooids are completely absent. The successive environmental belts from the proximal to the distal ramp are represented by facies associations FA1, FA3, FA8, FA5 and FA7.

The argillaceous peloidal very fine sands (Facies 8 packstone) form a prism, which pinches out seaward (Fig. 8). The planar upper surface of this prim is also an erosive surface. The flooding during the transgression and the associated hydrodynamic changes (razor effect, *sensu* Eichenseer & Leduc 1996) may explain this. Brachiopods are relatively common in these transgressive ooid-free facies, even in the inner part of the muddy ramp which confirms their preference for such open and moderately agitated environments (Almeras & Faure 1990; Almeras *et al.* 1994).

Aggrading oolitic interval. The physical correlation of stratigraphic beds shows progressively greater inclination of timelines upward (Fig. 8). The large scale aggrading and slightly prograding geometries of the depositional oolitic system during this stage are typical. During this interval, the lateral facies succession along these time lines from a proximal to a distal environment is FA1, FA2, FA4, FA5, FA6 and FA7 (Table 1). The transitions between all the facies zones are gradational and make discrete interpretation difficult. The ramp slope and therefore the proximal–distal dimension of the middle ramp facies belts evolve in this interval from 0.02° degrees and several kilometres to a maximum of 3° and few tens of metres.

Near the base of this unit and especially in the inner ramp domain, ravine surfaces are often observed. These irregular erosion surfaces mark a granulometric jump from fine facies below to coarse facies above the surfaces. They are interpreted as submarine erosion surfaces created by episodic high energy events probably created by hydrodynamic waves or tides. In the outer ramp domain, tempestites seem to be more important during this stage of inclined profile than at any other stage of ramp evolution. The outer ramp during this interval is also notable for the development of bioconstructional deposits (Facies 6b).

The carbonate production (e.g. ooids) is generally localized in tidal oolitic systems and in permanently wave-agitated areas of the mid-ramp. Meanwhile, the transition zone between lagoon and oolitic shoals is a place of accumulation of tidal and storm wash-over deposits (Facies 2d). Differential rates of sediment accumulation along the slope profile lead to progressively steepening depositional profiles during this time, shown on photos by stratal surfaces that reach 3–4° at the slope break.

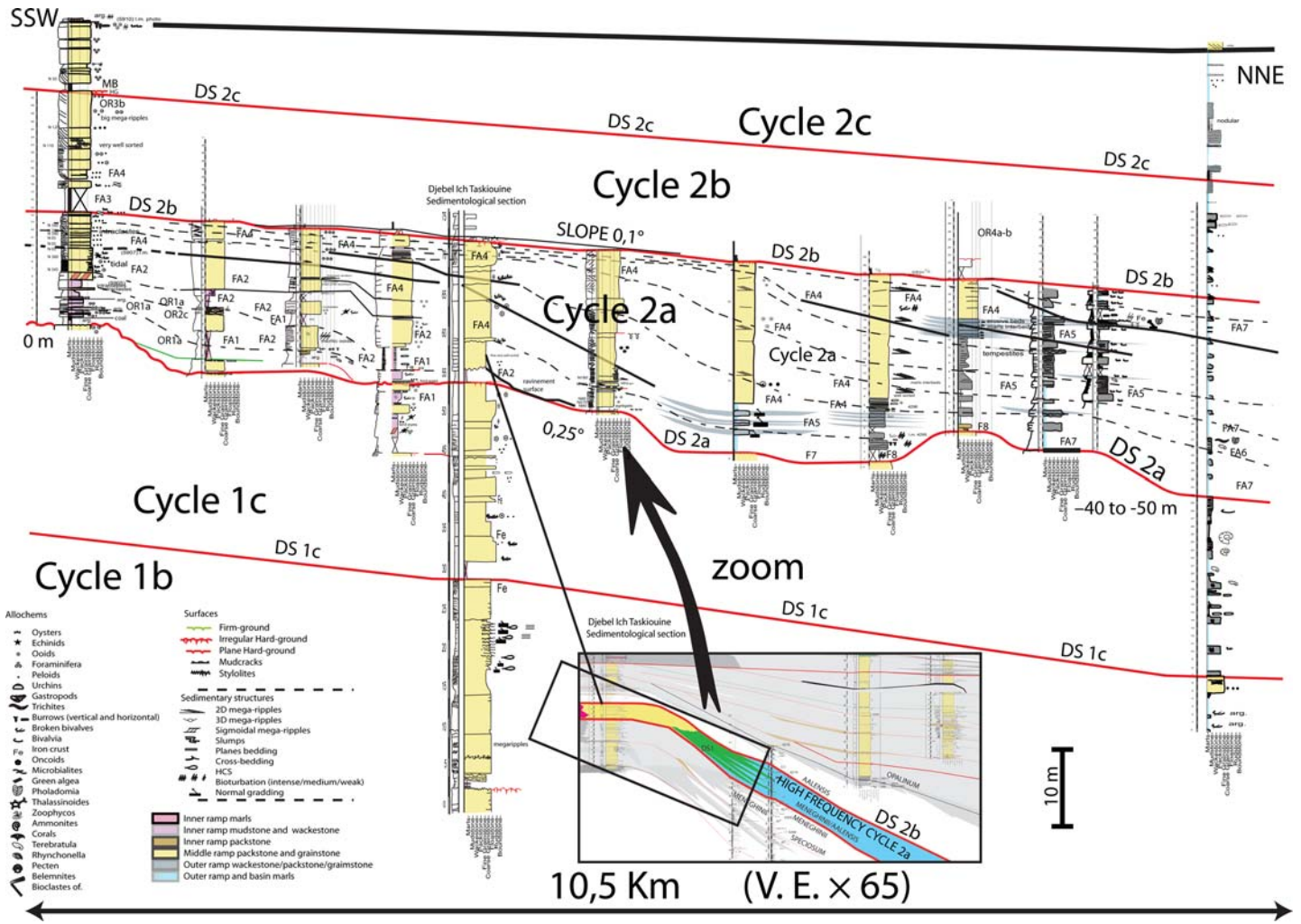

Fig. 8. Correlation panel showing the lateral distribution of facies and discontinuities and their time relationships within high-frequency cycles 2a. The evolution of the depositional model along timelines is deduced from these correlations.

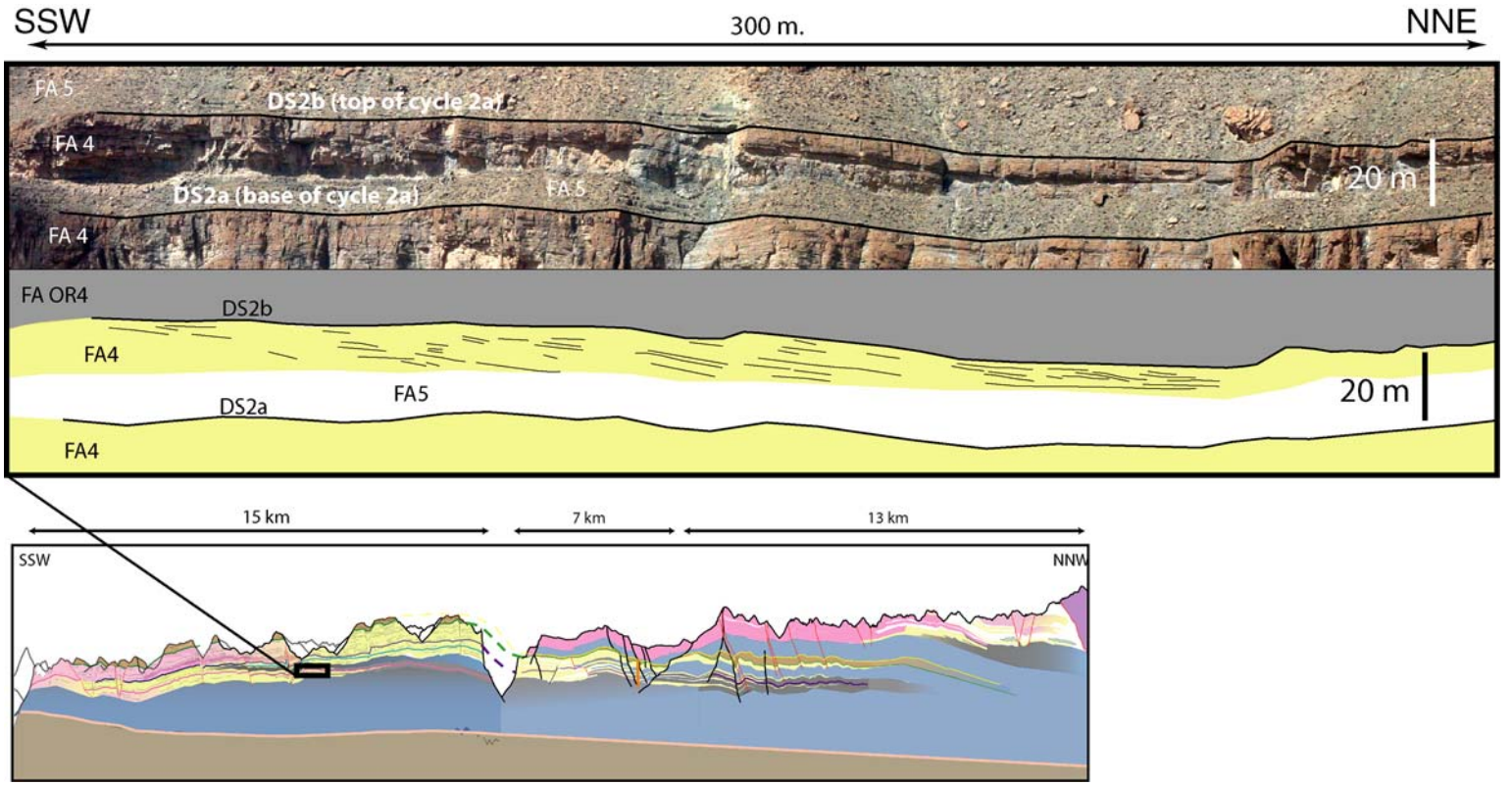

Fig. 9. Progradation of oobioclastic clinoforms.

Prograding oolitic interval. The physical correlation of beds shows that at the large scale, this interval is composed of prograding oobioclastic wedges. Such prograding wedges are mainly composed of low angle clinoforms with a maximum average slope of 3° (Fig. 9). The correlation of sedimentological sections as well as the analysis of photomosaics show that the facies succession along a time-line from proximal to distal environments is FA4, FA6 and FA7 (Figs 8 & 10). This succession includes ooid ramp facies; however, the restricted, proximal environments (FA1 and FA2) were either not deposited or not preserved. In addition, observed structures (cross beds, massive megaripples) in oolitic deposits reflect the most highly agitated hydrodynamic conditions within the high frequency cycle.

Interpretation of the cycle architecture. The high frequency cycles are composed of laterally shifting (or 'retreating', aggrading, and prograding) facies tracts. Each of these tracts is associated with a particular sedimentary system. A conceptual model that illustrates the main facies elements, geometries, and early diagenetic properties of the 26 elementary high frequency cycles is presented in Figure 10.

Transgression across a partially exposed platform. Based on the surface characteristics (early marine cementation, colonization by marine organisms) and the proximal facies observed below and the distal facies observed above, the basal discontinuity of the cycle is interpreted as the result of transgression across a partially exposed platform (Fig. 10).

Start up of the carbonate factory, low energy ramp. Ooids are completely absent across the entire ramp during the early transgression. From the most proximal environment to the hemipelagic basin, mudstone, peloidal, oncoidal wackestone, peloidal and intraclastic packstone and grainstone, and marls dominate the muddy ramp system (Fig. 10). The proximal facies are very close to those of the oolitic system, except that there are no backshore oolitic sands. All across the muddy ramp system, the high energy facies are rare. They mainly include bioturbated grainstone and packstone with peloids, benthic foraminifera, micritic intraclasts, wood debris and glauconitic grains. The facies variation between proximal and distal muddy facies is transitional and subtle. The distal muddy ramp environment is one of intercalated marl-limestone interlayered with tempestites. The latter is close to the oolitic outer ramp but with more pelloids and no ooids.

It appears that this ramp profile is very flat without any slope break. In contrast to the oolitic ramp system, this system is named 'muddy ramp system'. All the environments reflect weakly agitated hydrodynamic conditions that were not favourable for ooid formation. Hydrodynamic changes induced during initial transgression (the wave razor) lead to multiple erosive surfaces like the planar upper surface of the pelletoidal very fine sand shoals (Facies 8).

Higher accommodation, higher energy, aggrading ooid ramp. During the aggrading time interval, the ooid factory is restored and develops an oolitic ramp shoal (Fig. 10). The classic facies juxtaposition from inner ramp to the basin (Burchette *et al.* 1990; Burchette & Wright 1992; Badenas & Aurell 2001), the dimension of the facies belts and the depositional slope profile allow for the comparison with the present-day Persian Gulf Trucial Coast oolitic ramp systems (Loreau & Purser 1973; Loreau 1982).

Reducing accommodation, infill and progradation of high energy ooid belts. During this phase of the cycle, ooid grains dominated, leading to a major progradation of the sedimentary system. One of the most striking observations is the extensive progradation driven by a surge in ooid production probably coinciding with and linked to a decrease in accommodation space inferred from beds thinning upward (Fig. 8).

Low angle clinoforms and the partitioning of facies along a time line suggest that the belt of ooid production and/or deposition is narrow with a width less than 1 km. However, the lateral extension of the ooid facies bodies can reach more than 15 km (Fig. 3). Consequently, at the scale of the Amellago transect, these oolitic facies bodies are diachronous and the oolitic wedges are platform prisms which prograde and overlie the deep ramp deposits.

End of cycle. The inner ramp may have been partially exposed. The cycle ends with a new surface. This surface is similar in terms of shape and sedimentological characteristics to the basal surface. Both surfaces must have had the same origin. They are the result of a transgression across a partially exposed platform. Above this surface, a new ooid-free muddy ramp system develops. This story is repeated 26 times in the studied interval.

Comparison with the Persian Gulf

On the basis of modern oolitic systems from the Persian Gulf and British West Indies, some authors (Loreau & Purser 1973; Loreau 1982; Lloyd *et al.* 1987) suggest that ooid production and depositional belts are limited in width. Following this interpretation, the ancient, broad oolitic bodies could be the result of migration of the ooid factory or a

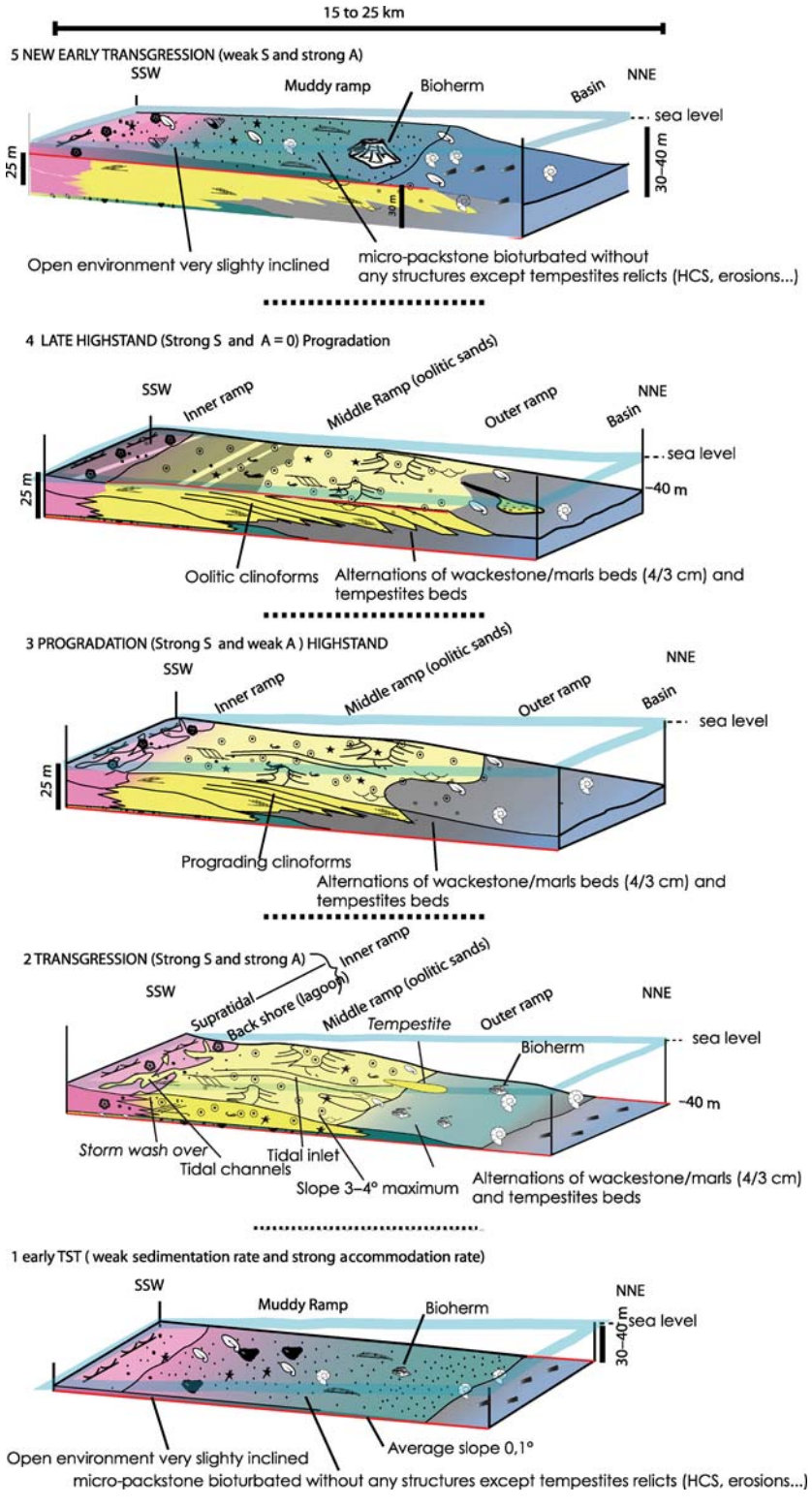

Fig. 10. 3D diagrams showing evolution of depositional environments.

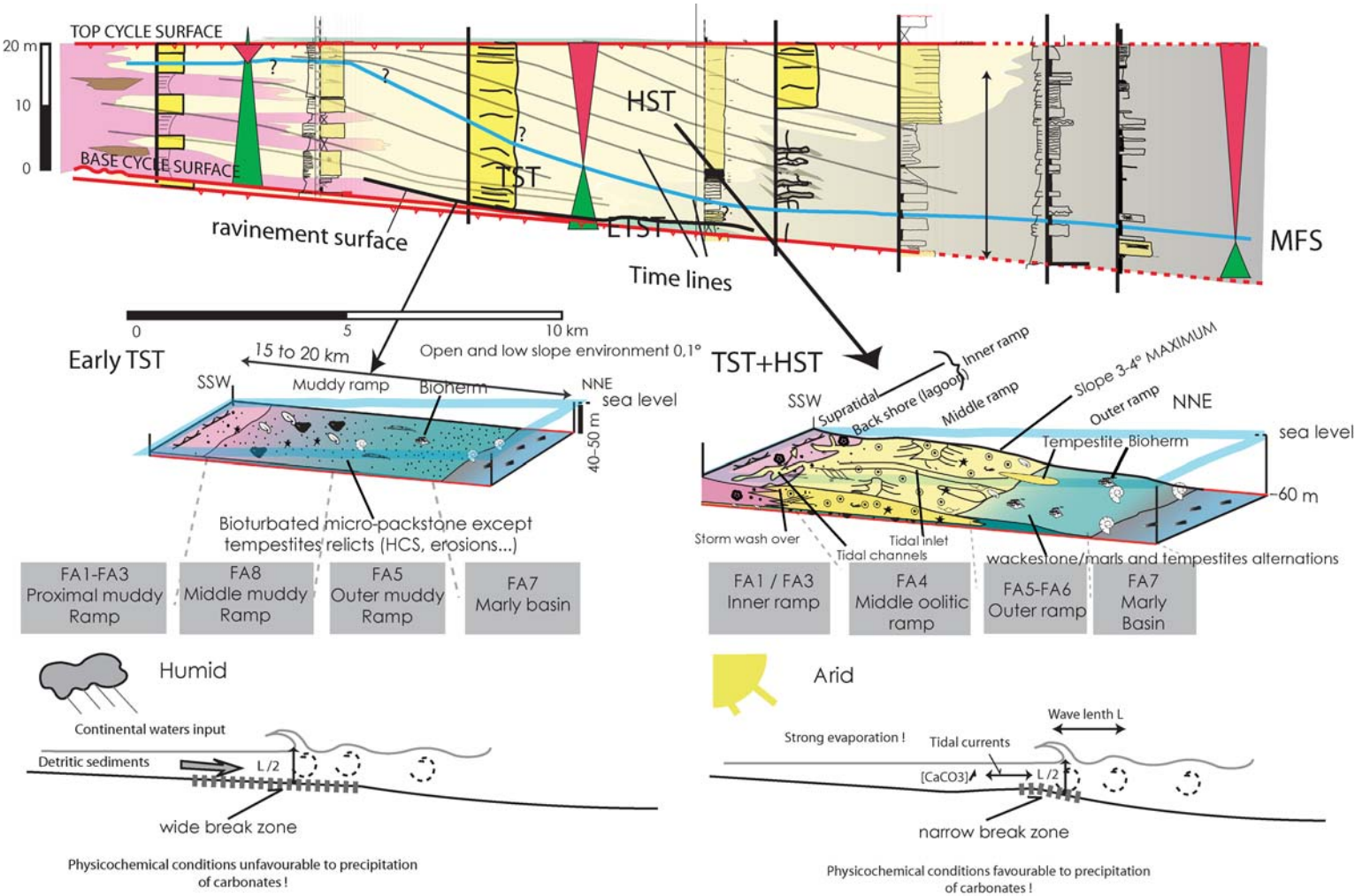

Fig. 11. 'Synthesis' with characteristics of the two different ramp depositional systems during high frequency cycles. During transgression, low carbonate production rates with a low angle, a muddy system is established. Whereas during late transgression to late highstand, a phase of high production rates with an ooid dominated higher angle ramp system is established.

redistribution of ooids from their production area. In the Holocene analogue of West Caicos, a beach and shoreface oolitic system can prograde over several kilometres in less than a million years and produce a sheet of oolitic sand averaging 5 m thick (Lloyd *et al.* 1987). The observations in recent environments and in the Amellago example presented here, suggest that continuous oolitic geobodies across great down-dip distances in other basins may be diachronous and the result of strong progradation and seaward migration of facies belts.

Discussion

The Amellago ramp system is characterized by high frequency cyclic alternations of muddy early transgressive and ooid-dominated late transgressive and highstand intervals (Fig. 11). Although ooid-dominated ramp systems are common (Burchette *et al.* 1990; Burchette & Wright 1992; Badenas & Aurell 2001), the presence of the muddy transgressive intervals has rarely been documented and may be linked to the specific factors controlling cyclicity at this ramp. For Strasser *et al.* (1999), climatic and eustatic cycles cannot be separated. The example of Kimmeridgian carbonate ramps of the Iberian Basin suggests that the relative sea-level changes are probably associated with climatic change and influenced the carbonate factory (Badenas *et al.* 2003, 2005). However, as Schlager (2005) mentioned, it is important to understand how these parameters act on a sedimentary system (e.g. sedimentary production change and morphology changes). The following sections discuss the relative influence of relative sea-level fluctuations and climatic changes on the high frequency cycles.

Eustacy-driven cyclicity

Relative sea-level variations are known to have a significant impact on ooid production by directly influencing hydrodynamics and sea-water chemistry. Since the early seventies, hydrodynamic agitation has been well known as a key factor in ooid formation (Bathurst 1971; Loreau & Purser 1973; Lucas *et al.* 1976; Loreau 1982; Tucker & Wright 1990). It stimulates seawater degasification and contributes to evaporation and air-bubble formation, which are processes that increase supersaturation and $CaCO_3$ precipitation (Girou 1970). Generally, ooid sands are abundant in such agitated environments while, in contrast, peloids are more common in calm environments.

All facies zones observed in the muddy ramp system reflect weakly agitated hydrodynamic conditions. The increase in ooid fraction of facies is coincident with the evolution of more steeply dipping depositional profiles. Schlager (2005) observed that ooids are more frequent during HST because tidal currents and wave action enhances their production. The influence of sea floor morphology on high-energy facies distribution was suggested by Purser (1983). During early transgression on the Amellago ramp, a very low angle depositional profile of about 0.01° was maintained and probably acted as a wide distal surf zone that would have dissipated all wave energy (Fig. 11). In addition, the low topographic relief and absence of any barrier such as ooid shoals is interpreted to have caused diminished tidal current strength, leaving the inner muddy ramp more exposed to the sea than the inner ooid ramp domain (Fig. 7c). Brachiopods are present in Facies 3 and indicate a more open marine condition (Almeras *et al.* 1994). As a result, salinity and carbonate saturation may have been lower due to a less evaporation than on a platform with a barrier. This, in turn, may have hindered ooid production.

Low amplitude relative sea-level variations were sufficient to drown the Amellago ramp with facies belts shifting several kilometres. Eustatic sea-level variations can be explained by climate changes linked to astronomical Milankovitch cycles that influence insolation patterns on Earth (Vail *et al.* 1991). These changing insolation patterns controlled the sea level during the Pleistocene 'ice-house' by repeated melting and formation of polar and continental ice caps (Strasser *et al.* 1999). During the 'greenhouse' of Toarcian, Aalenian, and Bajocian times, presence of continental and polar ice caps is still under debate (Hesselbo & Jenkyns 1998; Cobianchi & Picotti 2001; Hallam 2001; Immenhauser 2005). The thermal extension/contraction of the upper layer of the oceans, the thermal change of volume in the deep oceanic currents, and the capture of water in aquifers and lakes (Gornitz *et al.* 1982; Menard *et al.* 1995; Cazenave 1999; Miller *et al.* 2005) are others possible factors that may have led to sea-level changes of high frequency low amplitudes during the Lias–Dogger transition. However, the question remains whether a rapid eustatic drowning of the ramp and the associated topographic change of the sea-floor could have triggered the total disappearance of ooids during transgression.

Climate-driven cyclicity

Modern analogues in the Persian Gulf, West Caicos, and the Bahamas show that agitation is not the unique and only factor that controls ooid formation (Bathurst 1971; Loreau & Purser 1973; Lucas *et al.* 1976; Loreau 1982; Lloyd *et al.* 1987; Tucker & Wright 1990). In the Persian Gulf, the climate is hot and highly evaporative. Ooid

formation here is significantly controlled by physical-chemical parameters such as temperature, salinity, pH and concentrations of Ca, Sr, and Mg that control the thermodynamics and kinetics of $CaCO_3$ precipitation.

In Amellago, a constant thermal subsidence inherited from the post-rift period creates accommodation space (Ellouz *et al.* 2003). If this space created by subsidence is not filled in by sediments, the ramp would drown. Consequently, the transgressive surface and the development of the muddy ramp system would result from a climatically-controlled carbonate and ooid productivity crisis. During the return of more favourable climatic conditions, ooid production could resume and fill the empty accommodation space until the next climatic crisis. Therefore, ooid production could also be predominantly controlled by climatic cycles, particularly arid versus humid cyclicity.

In the Amellago case study, two observations support the hypothesis of a more humid climate during ooid-free intervals.

(1) Locally, terrigenous particles in the muddy ramp deposits form thin beds of sandstones with a dominant micritic and locally microdolomite rich matrix, which have been observed westward of the Amellago ramp, near the deltaic systems of the Central High Atlas (Ettaki *et al.* 2000; Ettaki & Chellaï 2005). Their occurrence in the Amellago area during ooid-free intervals could be the sedimentary signature of increased weathering of the Saharan Craton, probably during more humid climatic conditions. However, the presence of such terrigenous elements may also be the result of a change in the littoral drift trajectory when oolitic shoals and barriers were absent. Alternatively, clastic-rich intervals may represent lowstand or late highstand clastics that were reworked during the ensuing early transgression (e.g. Eichenseer & Leduc 1996; van Buchem *et al.* 2002).

(2) Coaly debris, though rare is present in the muddy ramp deposits. This may indicate the development of forests or mangroves during relative humid periods (Tucker & Wright 1990).

(3) Unfortunately, geochemistry (in particular $\delta^{18}O$ measurements on calcitic shells) cannot be used in the Amellago ramp system due to the burial history of this area; signatures are not preserved (Railsback & Hood 2001). As a result it is difficult to prove climatic versus eustatic control over the high frequency ramp system.

Conclusions

The analysis of the carbonate system of Amellago leads to the recognition and characterization of geometries and the internal architecture of Jurassic oolitic ramp deposits. These results are afforded by the exceptional, seismic-scale dimensions of the continuous outcrop (37 km long and 1000 m high) along the ramp's dip profile. Important insights include ramp slopes, palaeobathymetry (Table 1) and widths of facies belts estimated directly from the interpretation of a photo-mosaic profile. The detailed stratigraphic framework establishes that, at the large scale (several millions years and several hundred metres of thickness), sedimentary systems gradually shift from overall prograding oobioclastic ramps to overall retrograding 'muddy ramps' from the Toarcian–Aalenian transition through the entire Aalenian.

At the small-scale (high frequency order cycle), correlation of serial sedimentological sections shows that the ramp profile evolved though time with the following:

(1) The high frequency cycles are composed of laterally shifting (or retrograding, aggrading, and prograding) facies tracts. Each of these tracts is associated with a particular sedimentary system.

(2) The retreating period is represented by ooid-free muddy systems and their aggrading and prograding intervals are represented by oolitic ramp systems.

(3) The strong volumetric partitioning observed here suggests that continuous oolitic facies along great distances in other basins may be diachronous and the result of strong progradations and seaward migration of facies belts.

(4) Depositional slopes and the widths of facies belts evolve over the course of a high frequency cycle (from 0.02° and several kilometres to a maximum of 3° and few tens of metres for the defined 'middle ramp').

Cycles can be controlled directly by eustacy or more indirectly by variability in carbonate production, which is largely a function of climatic variations. It is believed that during the evolution of a cycle, ooid production progressively increases leading to a dramatic progradation of the sedimentary system.

This unique outcrop is a reference for oolitic ramp models at several scales.

This study is a project of 'Equipe Stratigraphie quantitative et diagenèse' UMR CNRS Biogéosciences 5561, Université de Bourgogne, France. Very special thanks to Y. Alméras, J.-L. Dommergues, S. Elmi, P. Neige, R. Bourillot and L. Rulleau for biostratigraphy. Warm and hearty thanks to C. Grelaud, J. Tranier, S. Védrine and M. Ousri for their help on the field. We are also glad to thank the Faculty of Sciences Semlalia (Marrakech) for the scientific and logistical help. During the final revision of the paper, we received helpful comments from J. Kenter, A. Saller, J. Hsieh, A. Reed and other Chevron colleagues. We also thank the reviewers for their very constructive comments.

References

AIGNER, T. 1985. Storm depositional systems. *In*: FRIEDMAN, G. M., NEUGEBAUER, H. J. & SEILACHER, A. (eds) *Lecture Notes in Earth Sciences*. Springer-Verlag, Berlin, 174.

AIT BRAHIM, L., CHOTIN, P. *ET AL.* 2002. Paleostress evolution in the Moroccan African margin from Triassic to Present. *Tectonophysics*, **357**, 187–205.

ALMERAS, Y. & FAURE, P. 1990. Histoire des brachiopodes liasiques dans la Téthys Occidentale: Les crises et l'écologie. *Les Cahiers de l'Institut Catholique de Lyon*, **4**, 1–12.

ALMERAS, Y., ELMI, S., MEKAHLI, L., OUALI-MEHADJII, A., SADKI, D. & TLILI, M. 1994. Biostratigraphie des Brachiopodes du Jurassique moyen dans le domaine atlasique (Maroc, Algérie). Contraintes environnementales et relation avec l'évolution verticale des peuplements d'ammonites. *Proceedings of the 3rd International Meeting on Aalenian and Bajocian Stratigraphy*, 25–31 May, 1994, Marrakech, 219–241.

ALMERAS, Y., FAURE, F., ELMI, S., ENAY, R. & MANGOLD, C. 2006. Zonation des brachiopodes du Jurassique moyen sur la marge sud de la Téthys occidentale (Maroc, Algérie occidentale): Comparaison avec la marge nord-téthysienne française. *Geobios*, **40**, 1–19.

ALSHARHAN, A. S. & KENDALL, C. G. S. C. 1986. Precambrian to Jurassic rocks of Arabian Gulf and adjacent areas: their facies, depositional setting and hydrocarbon habitat. *American Association Petroleum Geologists Bulletin*, **70**, 997–1002.

ALSHARHAN, A. S. & WHITTLE, G. L. 1995. Sedimentary – diagenetic interpretation and reservoir characteristics of the Middle Jurassic (Araej Formation) in the southern Arabian Gulf. *Marine and Petroleum Geology*, **12**, 615–628.

ARBOLEYA, M. L., TEIXELL, A., CHARROUD, M. & JULIVERT, M. 2004. A structural transect through the High and Middle Atlas of Morocco. *Journal of African Earth Sciences*, **39**, 319–327.

AURELL, M., BOSENCE, D. & WALTHAM, D. 1995. Carbonate ramp depositional systems from a late Jurassic epeiric platform (Iberian Basin, Spain): a combined computer modelling and outcrop analysis. *Sedimentology*, **42**, 75–94.

AURELL, M., BADENAS, B., BOSENCE, D. & WALTHAM, D. 1998. Carbonate production and offshore transport on a Late Jurassic carbonate ramp (Kimmeridgian, Iberian basin, NE Spain): evidence from outcrops and computer modelling. *In*: WRIGHT, V. P. & BURCHETTE, T. P. (eds) *Carbonate Ramps*. Geological Society, London, Special Publications, **149**, 137–161.

BÁDENAS, B. & AURELL, M. 2001. Proximal-distal facies relationships and sedimentary processes in a storm dominated carbonate ramp (Kimmeridgian, northwest of the Iberian Ranges, Spain). *Sedimentary Geology*, **139**, 319–340.

BÁDENAS, B., AURELL, M., RODRÍGUEZ-TOVAR, F. J. & PARDO-IGÚZQUIZA, E. 2003. Sequence stratigraphy and bedding rhythms of an outer ramp limestone succession (Late Kimmeridgian, Northeast Spain). *Sedimentary Geology*, **161**, 153–174.

BÁDENAS, B., AURELL, M. & GROCKE, D. R. 2005. Facies analysis and correlation of high-order sequences in middle–outer ramp successions: variations in exported carbonate on basin-wide $\delta^{13}C_{carb}$ (Kimmeridgian, NE Spain). *Sedimentology*, **2**, 1253–1275.

BATHURST, R. G. C. 1971. *Carbonate Sediments and their Diagenesis*. Elsevier, Amsterdam, 658.

BOURILLOT, R., NEIGE, P., PIERRE, A. & DURLET, C. 2008. Early-Middle Jurassic Lytoceratid ammonites with constrictions from Morocco: paleobiogeographical and evolutionary implications. *Palaeontology*, **51**, 597–609.

BREDE, R., HAUPTMANN, M. & HERBIG, H. G. 1992. Plate tectonics and intracratonic mountain ranges in Morocco – The Mesozoic–Cenozoic development of the Central High Atlas and the Middle Atlas. *Geologische Rundschau*, 81.

BURCHETTE, T. P. & WRIGHT, V. P. 1992. Carbonate ramp depositional systems. *Sedimentary Geology*, **79**, 3–57.

BURCHETTE, T. P., WRIGHT, V. P. & FAULKNER, T. J. 1990. Oolitic sandbody depositional models and geometries, Mississippian of southwest Britain: implications for petroleum exploration in carbonate ramp settings. *Sedimentary Geology*, **68**, 87–115.

CAZENAVE, A. 1999. Les variations actuelles du niveau moyen de la mer. *Comptes Rendus de l'Academie des Sciences – Series IIA – Earth and Planetary Science*, **329**, 457–469.

COBIANCHI, M. & PICOTTI, V. 2001. Sedimentary and biological response to sea-level and palaeoceanographic changes of a Lower–Middle Jurassic Tethyan platform margin (Southern Alps, Italy). *Palaeogeography, Palaeoclimatology, Palaeoecology*, **169**, 219–244.

DRAVIS, J. 1979. Rapid and widespread generation of recent oolitic hardgrounds on a high energy Bahamian platform, Eleuthera Bank, Bahamas. *Journal of Sedimentary Petrology*, **49**, 195–208.

DURLET, C., ALMERAS, Y., CHELLAI, E. H., ELMI, S., LE CALLONEC, L. & LEZIN, C. 2001. Anatomy of a Jurassic carbonate ramp: a continuous outcrop transect across the southern margin of the High Atlas (Morocco). *Géologie Méditerranéenne*, **28**, 57–61.

EL HARFI, A., GUIRAUD, M. & LANG, J. 2006*a*. Deep-rooted 'thick skinned' model for the High Atlas Mountains (Morocco). Implications for the structural inheritance of the southern Tethys passive margin. *Journal of Structural Geology*, **28**, 1958–1976.

EL HARFI, A., GUIRAUD, M., LANG, J. & CHELLAI, E. H. 2006*b*. Jurassic architectural model of the southern Tethys Palaeomargin as deduced from Cenozoic geodynamic evolution of the High Atlas Mountains of Morocco. *Africa Geoscience Review*, **13**, 1–40.

EICHENSEER, H. & LEDUC, J.-P. 1996. Automated genetic sequence stratigraphy applied to wireline logs. *Bulletin Recherche Exploration Production, Elf-Aquitaine*, **20**, 277–307.

ELLOUZ, N., PATRIAT, M., GAULIER, J.-M., BOUATMANI, R. & SABOUNJI, S. 2003. From rifting to Alpine inversion: Mesozoic and Cenozoic subsidence history of some Moroccan basins. *Sedimentary Geology*, **156**, 185–212.

ELMI, S. 1990. Les applications géodynamiques de la stratigraphie: l'histoire triasico-jurassique de la marge vivaro-cévenole (France, Sud-Est). *Journée Louis David: Documents des Laboratoires de. Géologie de la Faculté des Sciences Lyon*, 93–123.

ELMI, S., AMHOUD, H., BOUTAKIOUT, M. & BENSHILI, K. 1999. Cadre biostratigraphique et environnemental de l'évolution du paléorelief du Jebel Bou Dahar (Haut-Atlas oriental, Maroc) au cours du Jurassique inferieur et moyen. *Bulletin de la Société Géologique de France*, **170**, 619–628.

ETTAKI, M. & CHELLAÏ, E. H. 2005. Le Toarcien inférieur du Haut Atlas de Todrha–Dadès (Maroc): sédimentologie et lithostratigraphie. *Comptes Rendus Geosciences*, **337**, 814–823.

ETTAKI, M., CHELLAI, E. H., MILHI, A., SADKI, D. & BOUDCHICHE, L. 2000. Le passage Lias moyen – Lias supérieur dans la région de todrha – dadès: évènements biosédimentaires et géodynamiques (Haut-Atlas central, Maroc). *Comptes Rendus de l'Académie des Sciences, Series IIA – Earth and Planetary Science*, **331**, 667–674.

GIROU, A. 1970. Etude cinétique de la précipitation des carbonates de calcium en phase aqueuse. Thesis, Université de Toulouse.

GORNITZ, V., LEBEDEFF, S. & HANSEN, J. 1982. Global Sea Level Trend in the Past Century. *Science*, **215**, 1611–1614.

GRADSTEIN, F. M., GRADSTEIN, F. M., SMITH, A. G., BLEEKER, W. & LOURANS, L. J. 2004. A new Geologic Time Scale with special reference to Precambrian and Neogene. *Episodes*, **27**, 83–100.

Groupe Français d'Etude du Jurassique 1997. Biostratigraphie du Jurassique ouest-européen et méditerranéen: zonations parallèles et distribution des invertébrés et microfossiles. *In*: HANTZPERGUE, P. (ed.) *'Mémoires' Bulletin Centre Recherche Elf Exploration Production*.

HADRI, M. 1993. Un modèle de plate-forme carbonatée au Lias-Dogger dans le Haut-Atlas Central au nord-ouest de Goulmima, Maroc. PhD Thesis, Université Paris 11.

HALLAM, A. 2001. A review of the broad pattern of Jurassic sea-level changes and their possible causes in the light of current knowledge. *Palaeogeography, Palaeoclimatology, Palaeoecology*, **167**, 23–37.

HESSELBO, S. P. & JENKYNS, H. C. 1998. British lower Jurassic sequence stratigraphy. *In*: GRACIANSKY, P. C., HARDENBOL, J., JACQUIN, T., VAIL, P. R. & FARLEY, M. B. (eds) *Sequence Stratigraphy of European Basins*. SEPM. Special Publication, **60**, 561–581.

HEYDARI, E. 2003. Meteoric versus burial control on porosity evolution of the Smackover Formation. *AAPG Bulletin*, **87**, 1779–1797.

HOMEWOOD, P., GUILLOCHEAU, F., ESCHARD, R. & CROSS, T. A. 1992. Corrélations haute résolution et stratigraphie génétique: une démarche intégrée. *Bulletin Centre Recherche Elf Exploration Production*, **16**, 357–381.

IMMENHAUSER, A. 2005. High-rate sea-level change during the Mesozoic: new approaches to an old problem. *Sedimentary Geology*, **175**, 277–296.

LAVILLE, E. 1981. Rôle des décrochements dans le mécanisme de formation des basins d'effondrement du Haut Atlas marocain au cours des temps triasique et liasique. *Bulletin Société géologique de France*, **23**, 303–312.

LAVILLE, E. 1985. Evolution sédimentaire, tectonique et magmatique du bassin jurassique du Haut Atlas (Maroc). Thèse d'Université, Montpellier.

LAVILLE, E. 1988. A multiple releasing and restraining stepover model for the Jurassic strike-slip basin of the Central High Atlas (Morocco). *In*: MANSPEIZER, W. (ed.) *Triassic-Jurassic Rifting. Continental Breakup and Origin of the Atlantic Ocean and Passive Margins*. Developments in Tectonics, **22**. Elsevier, New York, 499–523.

LAVILLE, E., PIQUE, A., AMRHAR, M. & CHARROUD, M. 2004. A restatement of the Mesozoic Atlasic Rifting (Morocco). *Journal of African Earth Sciences*, **38**, 145–153.

LLOYD, R. M., PERKINS, R. D. & KERR, S. D. 1987. Beach and shoreface ooid deposition on shallow interior banks, Turks and Caicos islands, British West Indies. *Journal of Sedimentary Research*, **57**, 976–982.

LOMANDO, A. J. 1998. Application of modern carbonate depositional systems to reservoir geostatistics. American Association of Petroleum Geologists, Salt Lake City Annual Meeting, 17–20 May, AAPG, Tulsa, 87.

LOREAU, J.-P. 1982. Sédiments aragonitiques et leur genèse. *Mémoires du Muséum National d'Histoire Naturelle*, Paris, **47**.

LOREAU, J.-P. & PURSER, B. 1973. Distribution and ultrastructure of Holocene ooids in the Persian Gulf. *In*: PURSER, B. (ed.) *The Persian Gulf*. Springer-Verlag, Berlin, 279–328.

LOREAU, J. P. & DURLET, C. 1999. Diagenetic stratigraphy of discontinuity surfaces: an application to paleoenvironments and sequence stratigraphy. *Neues Jahrbuch fur Geologie und Palaontologie*, **1**, 381–407.

LUCAS, G., CROS, P. & LANG, J. 1976. *Les roches sédimentaires – Etude microscopique des roches meubles et consolidées*. Paris, Doin, 2.

MATTAUER, M., TAPPONIER, P. & PROUST, F. 1977. Sur les mécanismes de formation des chaînes intracontinentales. L'exemple des chaînes atlasiques du Maroc. *Bulletin Société géologique de France*, **7**, 521–526.

MENARD, Y., LEFEBVRE, M., ESCUDIER, P. & FU, L. 1995. Ocean and climate: a quantitative answer, TOPEX/POSEIDON. *Acta Astronautica*, **37**, 293–299.

MICHARD, A. 1976. Eléments de géologie marocaine. *Notes et Mémoires du Services Géologiques du Maroc*, 252–422.

MILHI, A., ETTAKI, M., CHELLAI, E. H. & HADRI, M. 2002. Les formations lithostratigraphiques jurassiques du Haut-Atlas central (Maroc): corrélations et reconstitutions paléogéographiques. *Revue de Paléobiologie, Genève*, **21**, 241–256.

MILLER, K. G., KOMINZ, M. A. *ET AL*. 2005. The phanerozoic record of global sea-level change. *Science*, **310**, 1293–1298.

MOORE, C. H. 2001. Carbonate reservoirs: porosity evolution and diagenesis in a sequence stratigraphic framework. *Elsevier, Development in Sedimentology*, **55**.

NIEBUHR, N. & JOACHIMSKI, M. 2002. Stable isotope and trace element geochemistry of Upper Cretaceous

carbonates and belemnite rostra (Middle Campanian, north Germany). *Geobios*, **35**, 51–64.

PIERRE, A. 2006. *Un analogue de terrain pour les rampes oolitiques anciennes. Un affleurement continu à l'échelle de la sismique (falaises jurassiques d'Amellago, Haut Atlas, Maroc).* PhD Thesis, Université de Bourgogne.

PIQUE, A. 1994. *Géologie du Maroc – Les domaines régionaux et leur évolution structurale*. Pumag.

PIQUE, A. & MICHARD, A. 1989. Moroccan hercynides: a synopsis. The paleozoic sedimentary and tectonic evolution at the northern margin of West Africa. *American Journal of Sciences*, **289**, 286–330.

POISSON, A., HADRI, M., MILHI, A., JULIEN, M. & ANDRIEUX, J. 1998. The central High-Atlas (Morocco). Litho- and chronostratigraphic correlations during Jurassic times between Tinjdad and Tounfite. Origin of subsidence. *Mémoires du Muséum National d'Histoire Naturelle*, **179**, 237–256.

PURSER, B. 1983. *Sédimentation et diagenèse des carbonates néritiques récents.* Cours de L'Ecole Nationale Supérieur du Pétrole et des Moteurs, 2, Editions Technip.

RAILSBACK, L. B. & HOOD, E. C. 2001. A survey of multi-stage diagenesis and dolomitization of Jurassic limestones along a regional shelf-to-basin transect in the Ziz Valley, Central High Atlas Mountains, Morocco. *Sedimentary Geology*, **139**, 285–317.

READ, J. F. 1985. Carbonate platform facies models. *AAPG Bulletin*, **69**, 1–21.

SADKI, D. 1992. Les variations de faciès et les discontinuités de sédimentation dans le Lias-Dogger du Haut-Atlas Central (Maroc): chronologie, caractérisation, corrélations. *Bulletin Société géologique de France*, **163**, 179–186.

SARIH, S., QUIQUEREZ, A., GARCIA, J. P., EL HARIRI, K., ALLEMAND, P. & CHAFIKI, D. 2007. Sédimentologie et quantification de la subsidence des séries liasiques dans le Haut Atlas Central marocain (coupe de Foum Zabel, Région de Rich). *Africa Geoscience Review*, **14**, 181–194.

SCHLAGER, W. 2005. *Carbonate Sedimentology and Sequence Stratigraphy*. SEPM Concepts in Sedimentology and Paleontology, **8**.

STRASSER, A., PITTET, B., HILLGARTNER, H. & PASQUIER, J.-B. 1999. Depositional sequences in shallow carbonate-dominated sedimentary systems: concepts for a high-resolution analysis. *Sedimentary Geology*, **128**, 201–221.

TUCKER, M. E. & WRIGHT, V. P. 1990. *Carbonate Sedimentology*. Blackwell Scientific Publications, Oxford.

VAIL, P. R., AUDEMARD, F., BOWMAN, S. A., EISNER, P. N. & PEREZ-CRUZ, C. 1991. The stratigraphic signatures of tectonics, eustasy and sedimentology: an overview. *In*: EINSELE, G., RICKEN, W. & SEILACHER, A. (eds) *Cycles and Events in Stratigraphy*. Springer-Verlag, Berlin, 617–659.

VAN BUCHEM, F. S. P., PITTET, B., HILLGARTNER, H., GROTSCH, J., AL MANSOURI, A. I., DROSTE, H. & OTERDOOM, W. H. 2002. High-resolution sequence stratigraphic architecture of Barremian/Aptian carbonate systems in northern Oman and the United Arab Emirates (Kharaib and Shu'aiba Formations). *GeoArabia*, **7**, 461–500.

WILMSEN, M. & NEUWEILER, F. 2008. Biosedimentology of the Early Jurassic post-extinction carbonate depositional system, central High Atlas rift basin, Morocco. *Sedimentology*, **55**, 773–807.